universität wien

DIPLOMARBEIT / DIPLOMA THESIS

Titel der Diplomarbeit / Title of the Diploma Thesis

„Studies on the biological activity of Bumetanide derivatives“

verfasst von / submitted by

Nina Ngoc Thanh Phan

angestrebter akademischer Grad / in partial fulfilment of the requirements for the degree of

Magistra der Pharmazie (Mag.pharm.)

Wien, 2019 / Vienna, 2019

Studienkennzahl lt. Studienblatt / degree programme code as it appears on the student record sheet:	A 449
Studienrichtung lt. Studienblatt / degree programme as it appears on the student record sheet:	Diplomstudium Pharmazie
Betreut von / Supervisor:	ao. Univ.-Prof. Mag. Dr. Thomas Erker

Danksagung

Allen voran möchte ich mich bei meiner Betreuerin Paola Martinelli, PhD für die Bereitstellung dieses Diplomarbeitsthemas bedanken sowie dafür, dass sie stets Zeit für die Beantwortung meiner Fragen fand. Bei ao. Univ.-Prof. Mag. Dr. Thomas Erker bedanke ich mich für die Möglichkeit, dass ich an diesem Projekt teilnehmen durfte.

Außerdem bedanke ich mich bei meinen Studienkolleginnen für die jahrelange gegenseitige Unterstützung, die vieles erleichtert hat, sowie dafür, dass die Studienzeit dank ihnen nicht nur aus Lernen bestand.

Zu guter Letzt möchte ich mich vor allem bei meiner Familie dafür bedanken, dass sie mir das Studium nicht nur finanziell ermöglicht haben, sondern mir auch in schwierigen Phasen dieser Zeit beigestanden sind, indem sie mich stets ermutigt und immer an mich geglaubt haben.

Table of contents

1 INTRODUCTION

1.1 Pancreas

1.1.1 Anatomy and function of pancreas [1]

The human pancreas is located in the abdominal cavity behind the stomach. It is divided into the head of pancreas, the body of pancreas and the tail of pancreas. The head of the pancreas is on the right side of the abdomen and is surrounded by the duodenum. The body lies behind the stomach and the tail of the pancreas is on the left side and abutting the spleen.

The pancreas is a secretory structure and contains two different glands:

- The exocrine gland has a role in food digestion and is secreting pancreatic juice into the intestines. The juice contains bicarbonate, which neutralizes the acids of chyme moving in from the stomach, as well as enzymes that helps digestion and absorption of nutrients from the food we eat. The enzymes are produced by the acinar cells and secreted into the ducts, which merge to form larger ducts and empty into the pancreatic duct. The pancreatic duct is connected to the bile duct, where the juice is released into the duodenum at the ampulla of Vater. Two major cell types compose the exocrine part of the pancreas: acinar cells, which produce and secrete the enzymes, and ductal cells, which form the network of ducts collecting and transporting the enzymes to the duodenum and secrete bicarbonate.
- A much smaller percentage of the cells in the pancreas are endocrine cells. Most of the endocrine cells in the pancreatic islets (or islets of Langerhans) are called the alpha- and beta-cells. They release insulin and glucagon into the blood, respectively, important hormones regulating glycaemia. Additionally, other populations of endocrine cells are present in the islets in smaller numbers.

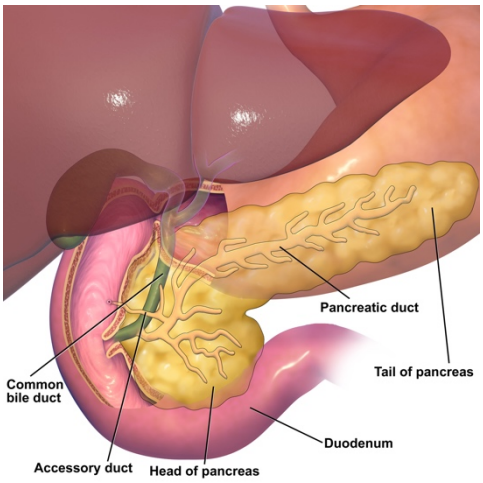

Figure 1: Anatomy of the pancreas [2]

1.1.2 Pancreatic cancer [1]

Pancreatic cancer arises when cells of the pancreas start to multiply out of control, although hyperproliferation can also be benign, in an early phase. Benign hyperproliferation might become cancer when it is left untreated.
There are different types of tumors in the pancreas. The exocrine cells form exocrine cancers and the endocrine cells form endocrine tumors. It is important to distinguish between this types of cancer. They have different risk factors, etiologies, signs, and symptoms. They are diagnosed with distinct test, treated in different ways and have different outcomes.
The most common type of pancreatic tumor, with about 85% of cases, is the pancreatic ductal adenocarcinoma (PDAC), an exocrine tumor which starts in the exocrine cells. Given its ductal-like appearance, it is thought to originate from ductal cells, but several lines of evidence from animal models suggest that it might also originate from acinar cells undergoing metaplastic processes.
Endocrine tumors are uncommon. They represent less than 4% of all pancreatic tumor cases. They are also known as neuroendocrine tumors (NETs) or islet cell tumors and are generally less aggressive than an adenocarcinoma. Pancreatic NETs can be either benign or malignant tumors. They can be divided into functioning tumors and non-functioning tumors.
Functioning tumors are pancreatic NETs which secret hormones such as insulin, glucagon and gastrin into the bloodstream, often in large quantities. The most common types of functioning NETs are insulinomas and gastrinomas, named after the hormones they secrete.
Non-functioning NETs do not secret enough hormones to cause overt symptoms. For this reason, they can grow quite large and spread into other parts of the body before they are diagnosed.
The major research topic of the lab is pancreatic ductal adenocarcinoma, therefore here we will focus on this type of pancreatic cancer.

1.1.3 Pancreatic Ductal Adenocarcinoma [3]

PDAC is not only the most common type of pancreatic cancer, but also the most aggressive. The survival rate for PDAC patients is only about 5-7%, and the median survival is roughly 6 months, numbers that have not significantly changed in the last 50 years.[4] Only a few demographic and social, as well as only a handful of autosomal dominant genetic risk factors associated with PDAC are known, which make the prevention very hard. The risk also seems to be elevated if one already had a PDAC case in the family. It is estimated that 10% of PDAC cases are based on inherited predisposition.

Germline mutations especially those which target the tumor suppressor genes INK4A, BRCA2, LKB1, the DNA mismatch repair gene MLH1 and the cationic trypsinogen gene PRSS1 are associated with familial PDAC.

PDAC more often starts in the head of the pancreas and can subsequently infiltrate into nearby tissues, including lymphatics, spleen, and the peritoneal cavity, and metastasize to the liver and lungs.

However, PDAC are observed also in the body and in the tail of the pancreas and the latter localization is associated with worse outcome. A prominent histopathological characteristic of pancreatic cancer is the so called desmoplasia, a dense stroma composed of fibroblasts and inflammatory cells. This particular microenvironment is considered to contribute to chemoresistance. Pancreatic stellate cells, which get activated in response to pancreatic injury, are a major component and driver of the desmoplastic reaction. Typical for PDAC is a glandular pattern with duct-like structures. Rarely seen is colloid, adenosquamous or sarcomatoid histology.

Related to PDAC there are three well known precursor lesions, which were identified in clinical and histopathologic studies:

- PanIN (pancreatic intraepithelial neoplasia)
- MCN (mucinous cystic neoplasm)
- IPMN (intraductal papillary mucinous neoplasm)

An adequate and common classification for precancerous lesions in pancreatic ducts is important for the harmonization of the international investigation on pancreatic carcinogenesis.

The most extensively studied precursor lesions are PanINs, which are found in the small ducts of the pancreas. Studies have shown that PanINs are a common finding in older patients without PDAC, with a frequency of up to 30% of specimens. PanINs are ranked into grade 1 to 3.
Stage 1 is characterized by columnar, mucinous epithelium. An increasing architectural disorganization and nuclear atypia is seen in the stages 2 and 3. PanINs of higher grade often transform into PDAC and invade beyond the basement membrane. Various molecular profiling studies have supported the PanIN-to-PDAC progression model.
Less common precursor lesions are MCNs and IPMNs. MCNs are located in body to tail and show no connection with the pancreatic ducts. MCNs are mucin-producing epithelial cystic lesions surrounded by a distinctive ovarian-type stroma, and are classified as adenoma, borderline and malignant lesions.
IPMNs look like PanINs in the cellular level but they often develop into larger cystic structures.

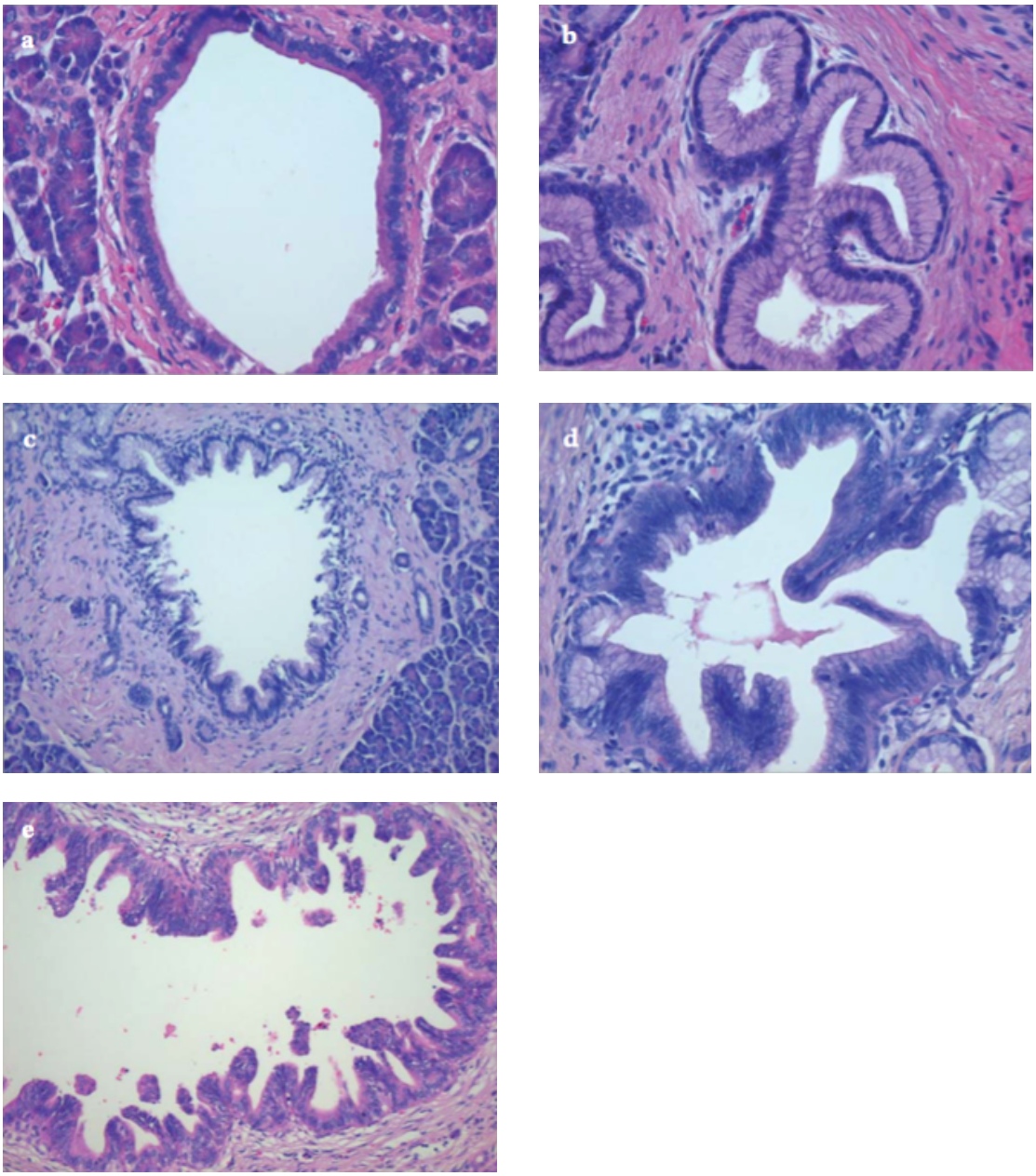

Figure 2a-2e [5]*:*

a. *Normal ductal epithelium: flat to cubic single-row epithelium without increased mucin production, basally, arrayed uniform nuclei without atypia).*

b. *PanIN-1A: single-row cylindrical epithelium with uniform basal cell nuclei and strong mucin production, no nuclear atypia. Very rare mitosis.*

c. *PanIN-1B: identical cell type as PanIN-1A, but with papillary, micropapillary or basal pseudostratified growth pattern.*

d. *PanIN-2: flat or papillary growth pattern of the epithelium, the nuclei have slight atypical signs such as nuclear size fluctuations, loss of polarity, pseudostratification and hyperchromaticity. Atypical mitoses, intraluminal glands, or cell debris in the lumen are not found).*

e. *PanIN-3: Cytologically, these lesions are already carcinoma cells, but there is no invasion of the basal membrane. The epithelia have severe atypical signs such as loss of nuclear polarity with lumen-displaced, enlarged, irregularly shaped, and highly hyperchromatic nuclei, which often have macronucleoli. Atypical mitoses may be present, and irregular intra-ductal irregular gland formation as well as necrosis are regularly detected) .*

1.1.4 Signs and symptoms [1]

Pancreatic cancer is often not diagnosed until it has already grown through the pancreas or spread into other parts of the body, because usually it does not cause specific symptoms or signs in early stages. This is the reason for the poor survival rates.
The common symptoms of pancreatic adenocarcinoma before diagnosis include:

- **Jaundice**, a yellowing of the eyes and skin, is one of the first symptoms people with pancreatic cancer will have. It is caused by the accumulation of a dark yellow-brown substance called bilirubin. Bilirubin is made in the liver and goes through the common bile duct into the intestines. Bilirubin accumulates in the body when the common bile duct is blocked.
  This happens when the cancer reaches the head of the pancreas and obstructs the common bile duct while it grows through the pancreas.
  Other signs of jaundice are darkened urine, light-colored stools and itchy skin.

- **Abdominal pain** or back pain is caused because of the growth of the tumor in the pancreas. The pancreas can become fairly large and press on the other organs, causing pain. From the location of the pain you can say where the cancer is located.

- **Unintended weight loss** caused from loss of appetite or impaired exocrine function.

- **Digestive problems** result when the tumor presses on neighboring organs, disturbing digestive processes and causing nausea, vomiting and the feeling of fullness. Undigested fat leads to unusually pale, greasy and foul-smelling stools.

- Pancreatic cancer can cause **diabetes** since the cancer destroys the insulin-making cells.

Other signs of pancreatic cancer can be gallbladder enlargement, blood clots and fatty tissue abnormalities. However, none of the symptoms mentioned above is really specific for pancreatic cancer, therefore it can be difficult to properly diagnose it when it is in its early stages and could be surgically removed. This is one of the reasons for the dismal prognosis.

1.1.5 Molecular genetics of PDAC

Evolving PDAC shows typical genetic lesions, which involve known cancer genes and classical cancer signaling pathways. These molecular events are classically linked with defined histopathological stages of PDAC progression. The major question is how these mutations contribute to the biological features of the neoplasm [3].

The first data collected to this disease were K-RAS mutations, which show a high incidence in pancreatic cancer. The frequency of these mutations can be up to 95% in PDAC patients and K-RAS mutations are even reported in healthy pancreatic tissue. Furthermore, the frequency of occurrence increases with the stage of neoplasia, being 36% for PanIN-1A, and up to 87% in PanIN-2 or -3. Mutations in the K-RAS oncogene are thought to be the initiating event in PDAC [3].

The loss of the p53 tumor suppressor gene, especially in later stages of PanINs, plays a significant role. Missense changes in the DNA-binding domain are found in > 50% of PDAC cases. The loss of p53 can be attributes to an accumulation of genetic damage, such as telomere erosion.

Another tumor suppressor that is frequently lost during PDAC-progression is SMAD4 (DPC4) transcriptional regulator, which serves as a central component in the transforming growth factor – (TGF-)β-signaling cascade. In about 50% of PDAC cases, the SMAD4-gene is targeted for deletion or intragenic point mutations and was classified as a PDAC progression allele due to its loss in later PanINs, although the impact of SMAD4 loss on the PDAC prognosis has not yet been clearly established [3].

Germline mutations of the CDNK2A tumor suppressor gene have been implicated in patients with PDAC but also in patients with melanoma. Several studies have

determined that the incidence of PDAC and melanoma in the same patient indicates a congenital susceptibility to cancer and that in some cases this predisposition also results from germline CDKN2A mutations [6].
Other mutations during carcinogenesis involve the BRCA2-tumor suppressor gene.
Other genetic alterations observed in PDACs and considered to be early events include overexpression of HER2/neu and shortening of telomeres [3].

1.1.6 Staging [1]

Before choosing treatment options it is important to stage the pancreatic cancer. The most common method for staging a cancer is the TNM staging system by the American Joint Committee on Cancer (AJCC). It is based on 3 key information:

- T: stands for the size of the main tumor
- N: describes the spreading to nearby lymph nodes
- M: indicates if the cancer has metastasized to other organs

Following numbers and letters after T, N and M provide more details about these factors.

1.2 Bumetanide and NKCC1

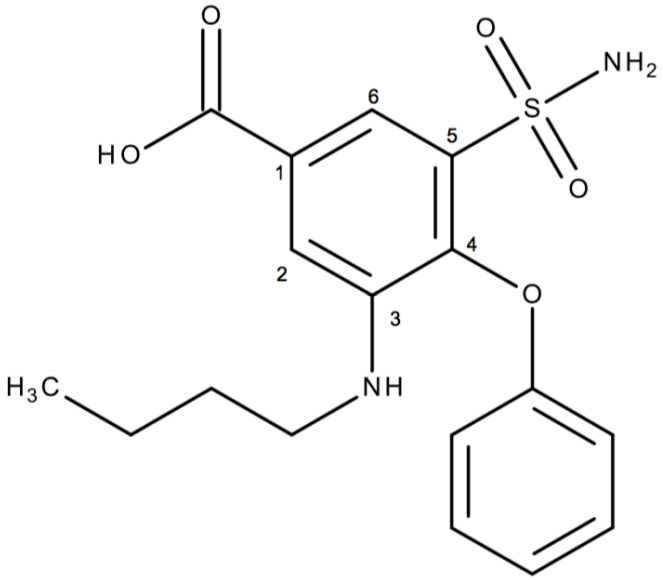

Scheme 1: Chemical structure of bumetanide.

Bumetanide belongs to a drug class called loop diuretics drug. It is a fast-acting, but short in its duration of action, saludiureticum. Bumetanide has the molecular formula C17H20N2O5S and a molar mass of 364.42 g / mol. It is used to treat heart failure, nephrotic syndrome, renal insufficiency and liver cirrhosis (prevention of edema). The mechanism of action is the inhibition of the Na-K-2Cl (NKCC)-cotransporter in the rising part oft he Henle loop [7].

The Na-K-2Cl cotransporter is a protein that serves to absorb sodium, potassium and chloride. It is an electroneutral transport protein. There are two isoforms of NKCC.

NKCC1 can be found ubiquitously in all body cells, but especially in ducts of glands and only during embryogenesis. As a result of its activity, the effect of the neuronal reaction on γ-aminobutyric acid (GABA) and glycine changes from activating to inhibiting.

NKCC2 is restricted to the kidney. It serves in the ascending part of the Henle loop to re-absorb the sodium and concentrate the urine [8].

In this thesis we focus an NKCC1, which is also expressed in the exocrine part of the pancreas and known for its sensitivity to bumetanide. For this purpose, we used two different pancreatic cancer cell lines.
Figure 3 shows the expression of the *SLC12A1* gene, coding for NKCC1, in normal tissues. SLC12A1 is highly expressed in some tissues, such as sun-exposed skin or the brain, and only low expression is detected in the normal pancreas.

However, SLC12A1 expression is up-regulated in PDAC compared with normal tissue, which could be a tumor specific effect, as shown in Figure 4. This is the reason why pancreatic cancer cells where chosen for this thesis.

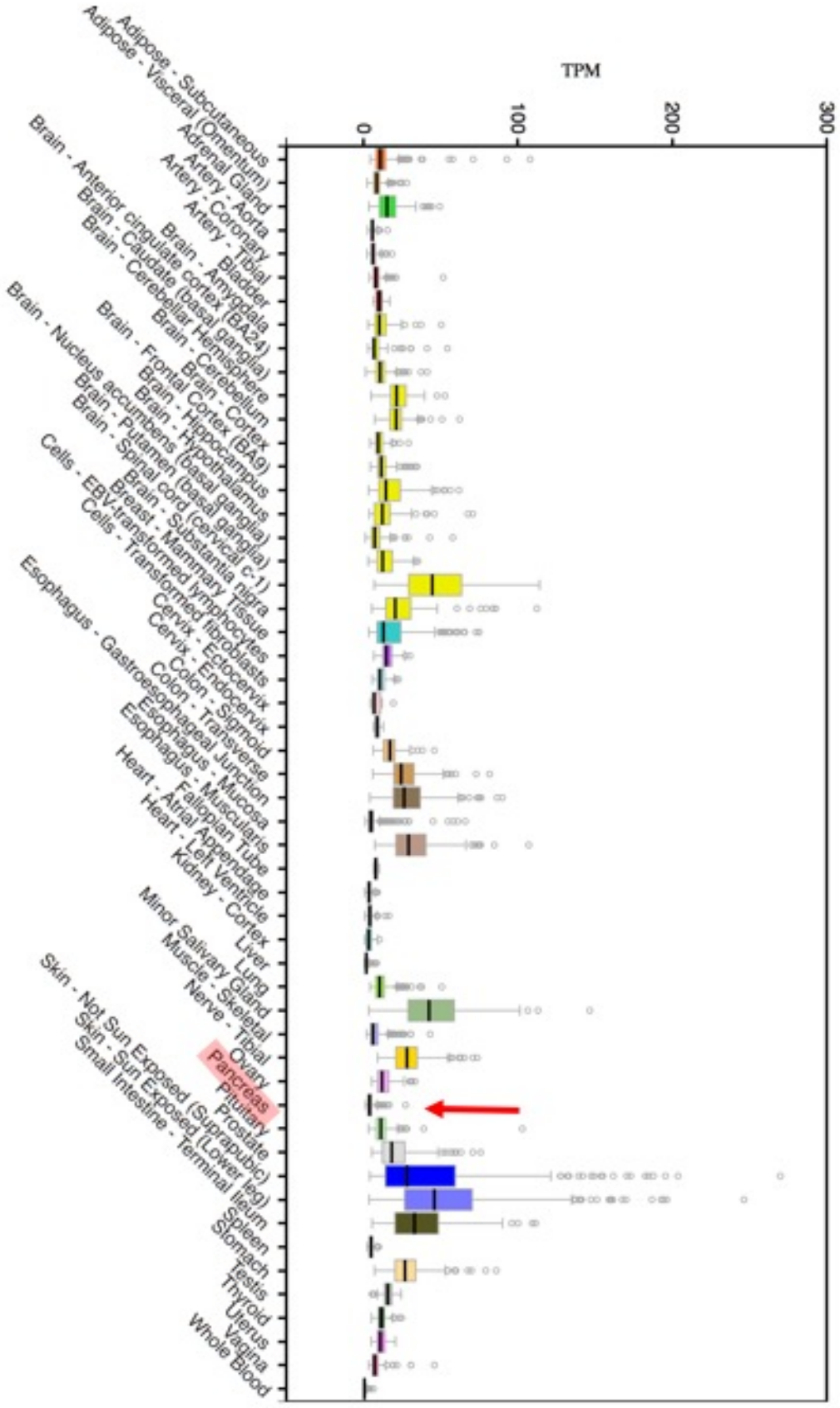

Figure 3: Expression of SLC12A1 in different healthy tissues [9].

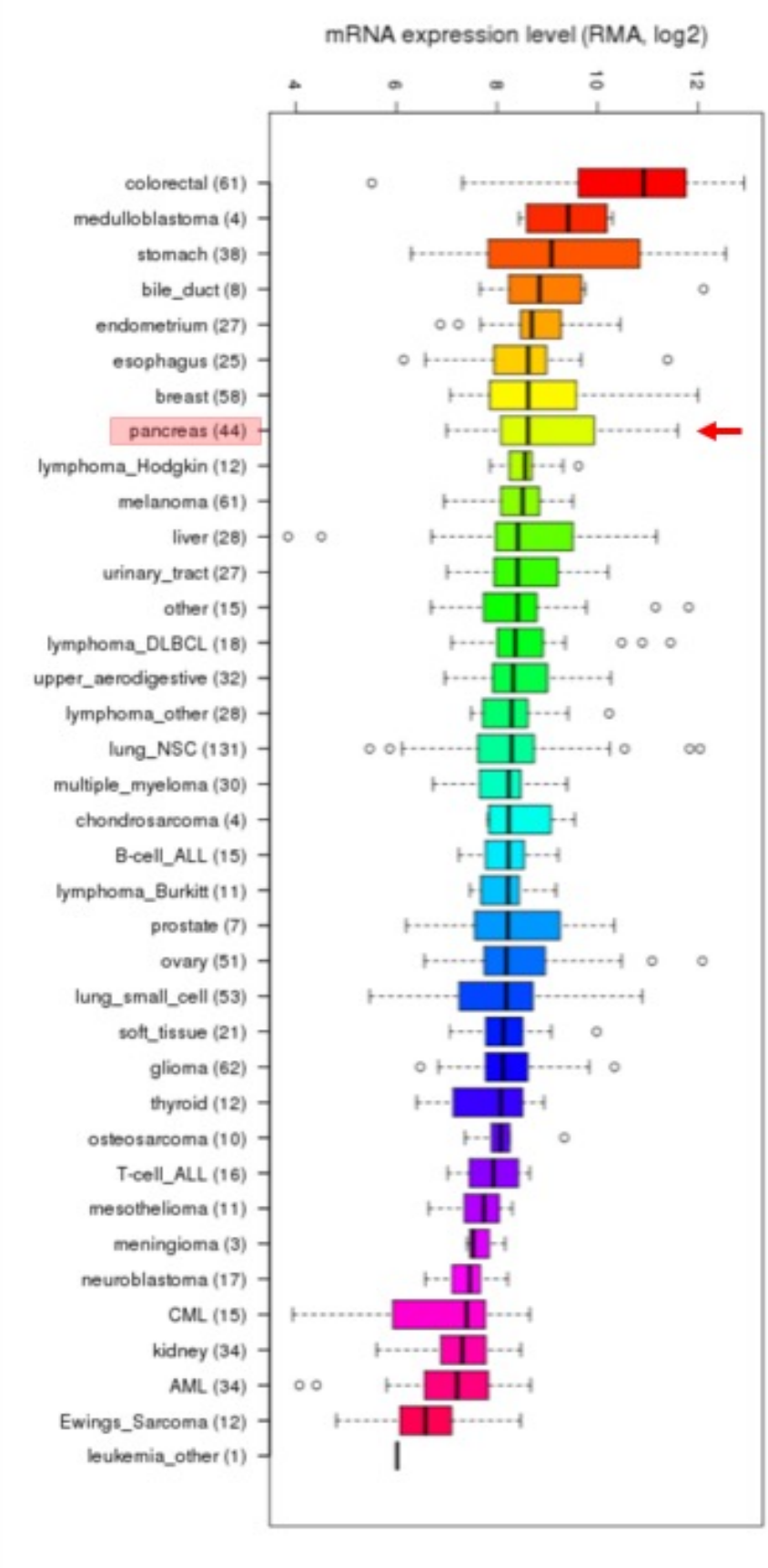

Figure 4: Expression of SLC12A2 in cancer tissues.

1.3 Drugs

1.3.1 Gemcitabine

The drug gemcitabine (2',2'-difluoro 2'-deoxycytidine, GEM) is the first-line chemotherapeutic agent for pancreatic cancer treatment [10]. It is the most important analogue of cytidine since cytosine arabinoside (Ara-C). Its antitumor activity has been confirmed in a series of *in vitro* and *in vivo* tumor models. Even though GEM is similar to Ara-C, it shows characteristic features. After the influx into the cell through nucleoside transporters, GEM converts to the nucleotides gemicitabine diphosphate (dFdCDP) and gemcitabine triphosphate (dFdCTP) [11]. GEM targets DNA synthesis, impairs DNA repair and induces apoptosis [10]. Even though GEM treatment results in inhibition of pancreatic cancer cell growth *in vitro*, its clinical efficacy remains low [12].

1.3.2 Paclitaxel

Paclitaxel (PTX) is another chemotherapy medication that is used to treat a number of cancer types, including ovarian cancer, breast cancer, lung cancer, Kaposi sarcoma, cervical cancer and pancreatic cancer.
PTX increases the polymerization of tubulin and interacts also with microtubule directly. With PTX the microtubule cytoskeleton is reorganized. It stabilizes the microtubule polymer and prevents it from degrading. The cells are blocked in G2/M phase and are unable to form a normal mitotic spindle which leads to apoptosis [13].

1.3.3 5-Fluorouracil

The drug 5-fluorouracil (5FU) is widely used for the treatment of cancer, particularly for colorectal cancer. It is an analogue of uracil, but instead of a hydrogen at the C-5 position there is a fluorine.
Its anticancer effects are based on the inhibition of thymidylate synthase and incorporation of the metabolites into DNA and RNA. 5FU is entering the cell with the same transport mechanism as uracil. It is converting into serveral active

metabolites like fluorodeoxyuridine monophosphate (FdUMP), fluorodeoxyuridine triphosphate (FdUTP) and fluorouridine triphosphate (FUTP). The metabolites interrupt RNA synthesis and action of thymidylate synthase, which causes DNA and RNA damage.

Due to its effect on RNA synthesis, 5FU can affect also non-proliferating normal cells and therefore it shows a rather strong toxicity. For this reason, and since it did not improve significantly the outcome when compared to GEM, its use for pancreatic cancer patients has been limited in the last years.

2 AIM OF THESIS

Pancreatic cancer is one of most deadly cancer types. It has an overall 5-year survival rate of 5%. Even though the knowledge about this disease has increased over the past few years, there is just limited progress on improving the survival of patients. Surgery it the only curative option for patients with pancreatic cancer, and is normally followed by adjuvant chemotherapy. However, most patients have an unresectable tumor already at the time of diagnosis, and receive mostly palliative chemotherapy.
Late stages of pancreatic cancer with metastasis make conventional treatment methods rarely successful. At the moment, chemotherapy with GEM, PTX or combinations of both are the most effective medications to improve survival. As mentioned above, 5FU is not superior to GEM and is more toxic, therefore it is not used very often, but still included in the FOLFIRRINOX combination (FOLinic acid, Fluorouracil, IRInotecan, OXaliplatin), which is given in the adjuvant and neoadjuvant setting to patients in good conditions.
One reason for the poor prognosis is that pancreatic cancer is often diagnosed at an advanced stage, because early stages of pancreatic cancer are usually asymptomatic. In addition to that, no effective screening tests are available for this disease. Also drug-resistance makes the search for other drugs urgent.

The central aim of the thesis is to show whether bumetanide derivatives (PTPs) can inhibit the growth of pancreatic cancer cells and through which mechanism(s).

As mentioned above bumetanide is a loop diuretic, which inhibits the NKCC1-cotransporter in the rising part of the Henle loop. The derivatives mainly differ in one side chain. By changing this chain, the function of bumetanide can be severely altered.

Furthermore, we seek to determine whether the sensitivity of pancreatic cancer cells to bumetanide derivatives depends on the expression of the NKCC1-transporters.

In addition, we will investigate whether the bumetanide derivatives show a synergistic effect with the drugs GEM, 5-FU and PTX.

3 MATERIALS AND METHODS

3.1 Test substances

The derivatives used in these experiments are:

- **PTP1 (BUM66)**, dissolved in DMSO
- **PTP2 (BUM5.HCl)**, dissolved in DMSO
- **PTP3 (BUM581.HCl)**, dissolved in DMSO

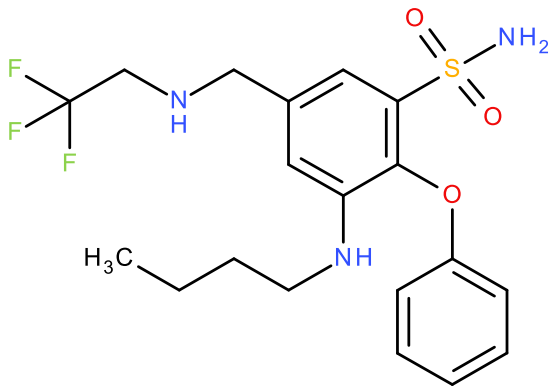

Scheme 3: Chemical structure of PTP1

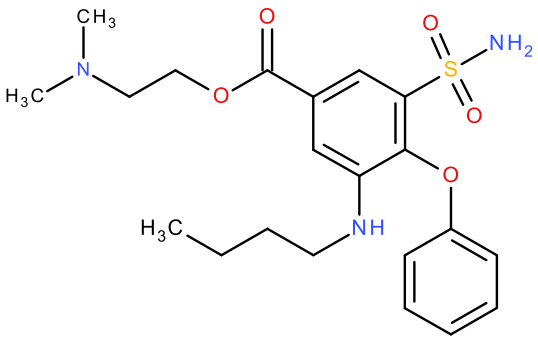

.HCl

Scheme 2: Chemical structure of PTP2

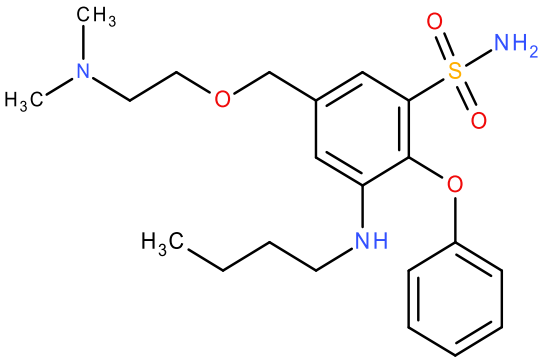

*HCl

Scheme 4: Chemical structure of PTP3

They were combined with the following cytostatics:

- **Gemcitabine (GEM)**, dissolved in DMSO
- **5-Fluorouracil (5FU)**, dissolved in DMSO
- **Paclitaxel (PTX)**, dissolved in DMSO

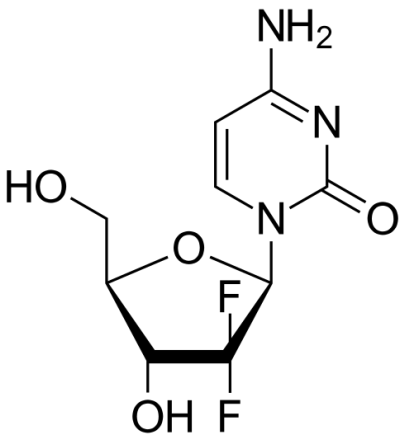

Scheme 7: Chemical structure of Gemcitabine,

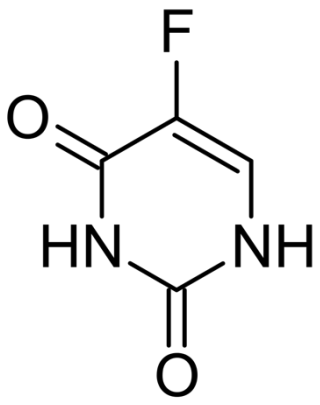

Scheme 5: Chemical structure of 5-Fluorouraci.

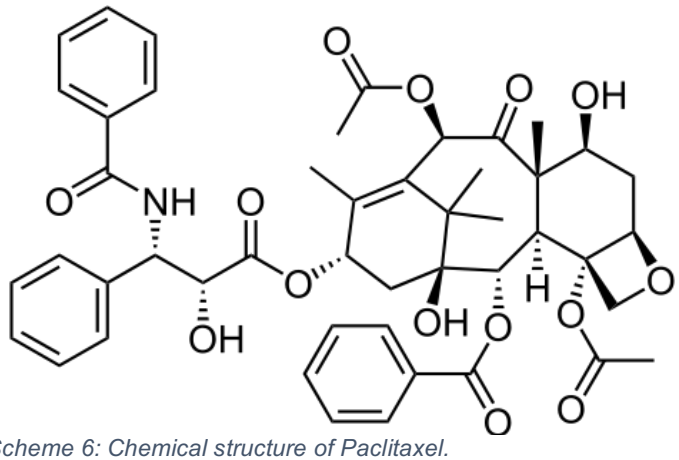

Scheme 6: Chemical structure of Paclitaxel.

PTP1, PTP2 and PTP3 were synthesized by the research group of Ao. Univ.-Prof. Mag. pharm. Dr. Thomas Erker at the department of pharmaceutical chemistry at the University of Vienna, Austria.

GEM, PTX and 5FU were purchased from Sigma-Aldrich, Austria.

The solutions were stored at -20°C.

Concentrations ranging from 100pM to 100µM were used for all drugs, as specified in each experiment.

3.2 Cell lines and culture medium

The substances were tested in cells on the PANC1 cell line (obtained from ATCC) and PaTu8988S (PatuS) cell line (gift from M. Buchholz at the University of Marburg, Germany).
Both cell lines were available at the Institute for Cancer Research in Vienna, but they are commercially available. Their tissue of origin was primarily pancreatic ductal adenocarcinoma.
Both cell lines express the gene *SLC12A2*, which encodes for the NKCC1-cotransporters.
The cells were maintained in Dulbecco's Modified Eagle's Medium (DMEM), supplemented with 10% fetal bovine serum (FBS) and 1% penicillin/streptomycin (P/S) (all of them purchased from Sigma-Aldrich, Austria). P/S is a solution stabilized with penicillin and streptomycin and is used to supplement cell culture medium to control bacterial contamination.

The medium was stored at 2 to 8 °C and was pre-warmed in a 37 °C water bath before use.

3.3 Cell culture

3.3.1 Thawing frozen cells

Both cell lines were long-term stored in freezing medium (FBS/DMSO 10%) in liquid nitrogen or in a freezer at -80 °C (short-term storage). DMSO acts as a cryoprotective agent and this way, the cells can be preserved for a long time. Frozen cells were thawed in a 37 °C water bath and transferred to a 15ml falcon with 5ml pre-warmed medium. Since DMSO is harmful to the cells, the cells were centrifuged at 1200 U/min for 5min at room temperature to get rid of it. The medium was aspirated and the cells were suspended in 7ml medium and plated onto 10cm dishes. To reproduce the same conditions of the human body, the cells were maintained in an incubator which was set at 37 °C and an atmosphere of 5% CO_2.

3.3.2 Splitting the cells

To maintain cell proliferation, passaging is necessary. PatuS cells, as well as PANC1 cells are adherent to the surface of the dish, and should always be subcultured before they reach confluency. They were detached with an enzymatic reaction: after removing the medium and washing the cells with Dubecco's Phosphate Buffered Saline (purchased from Sigma-Aldrich, Austria), 1 to 2ml of 0,25% trypsin-EDTA solution (purchased from Sigma-Aldrich, Austria) were added. The cells were incubated at 37°C until they detached (about 5 minutes). Detachment of the cells was checked under the microscope. By adding fresh culture medium, the trypsinization was stopped, thanks to the inhibitory effect of FBS-contained proteins. The cell suspension was thoroughly mixed and a part of the cells (subcultivation ratio of 1:2 to 1:4) was transferred into a new dish and filled up to 7 to 8ml with medium again. The other part was discarded.

3.3.3 Cell counting

For the experiments described below it was necessary to determine the cell number.
Therefore, the cells were detached from the dish as described and were transferred into a 15ml falcon. A sample of 10µl of cell suspension was mixed with 10µl of a 0,4% solution of trypan blue (purchased from Sigma-Aldrich, Austria) by pipetting.

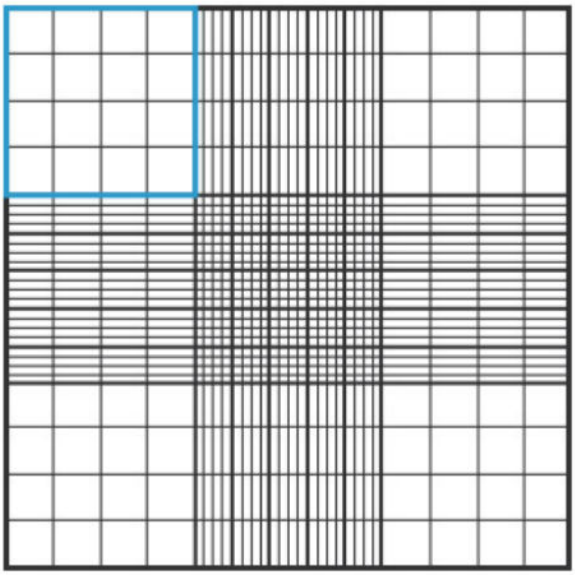

Figure 5: Hemocytometer-gridlines [14].

Trypan blue is an anionic azo dye used to stain dead tissues or cells. It is used for the assessment of the viability of cells. Living cells with intact cell membranes cannot absorb Trypan blue, whereas it is absorbed by dead cells, which appear blue under the microscope [14].

10µl of this suspension were applied to the hemocytometer until the chambers underneath the coverslip were filled.

Three of the sets of 16 squares (Figure 5: the blue line indicates one square) were used for counting, always taking three sets diagonally to each other. The cells were counted under the microscope according to the pattern in Figure 6. Cells touching the upper and left edge were included, whilst cells lying on the right and lower edge were excluded.

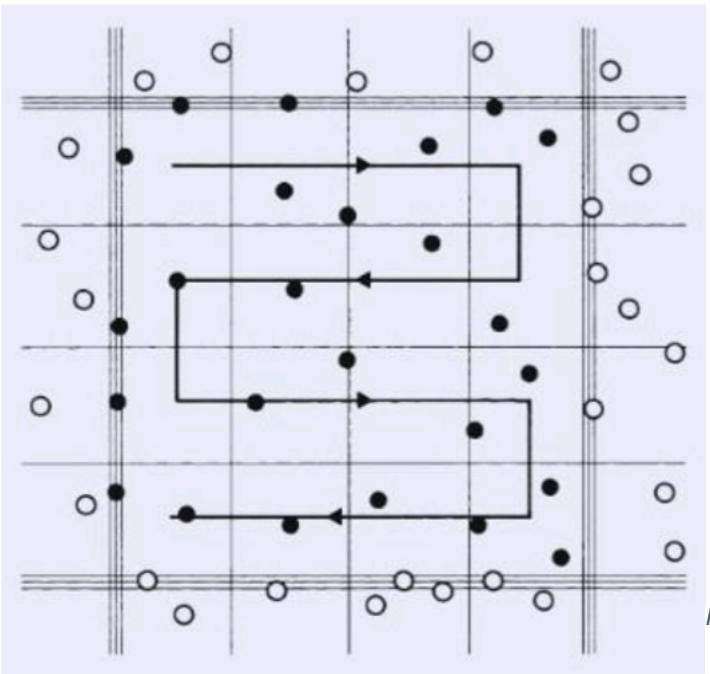

Figure 6: Counting pattern in a hemocytometer. [24].

Cells that absorbed trypan blue must not be counted, as they are non-viable. The total number of counted cells was divided by three to have the average. The average was then multiplied by 2, since the cell suspension had been diluted 1:1 with trypan blue solution. The resulting value is multiplied by 10^4 (a constant depending on the hemocytometer size). The result is the approximate number of cells per ml.

3.4 Cytotoxicity assay

3.4.1 Procedure

Cells were seeded in 96-well plates at a density of $5x10^3$ cells/well. Twenty-four hours later the medium was replaced with 0,1ml or 0,2ml fresh medium containing the test substances in desired concentrations.

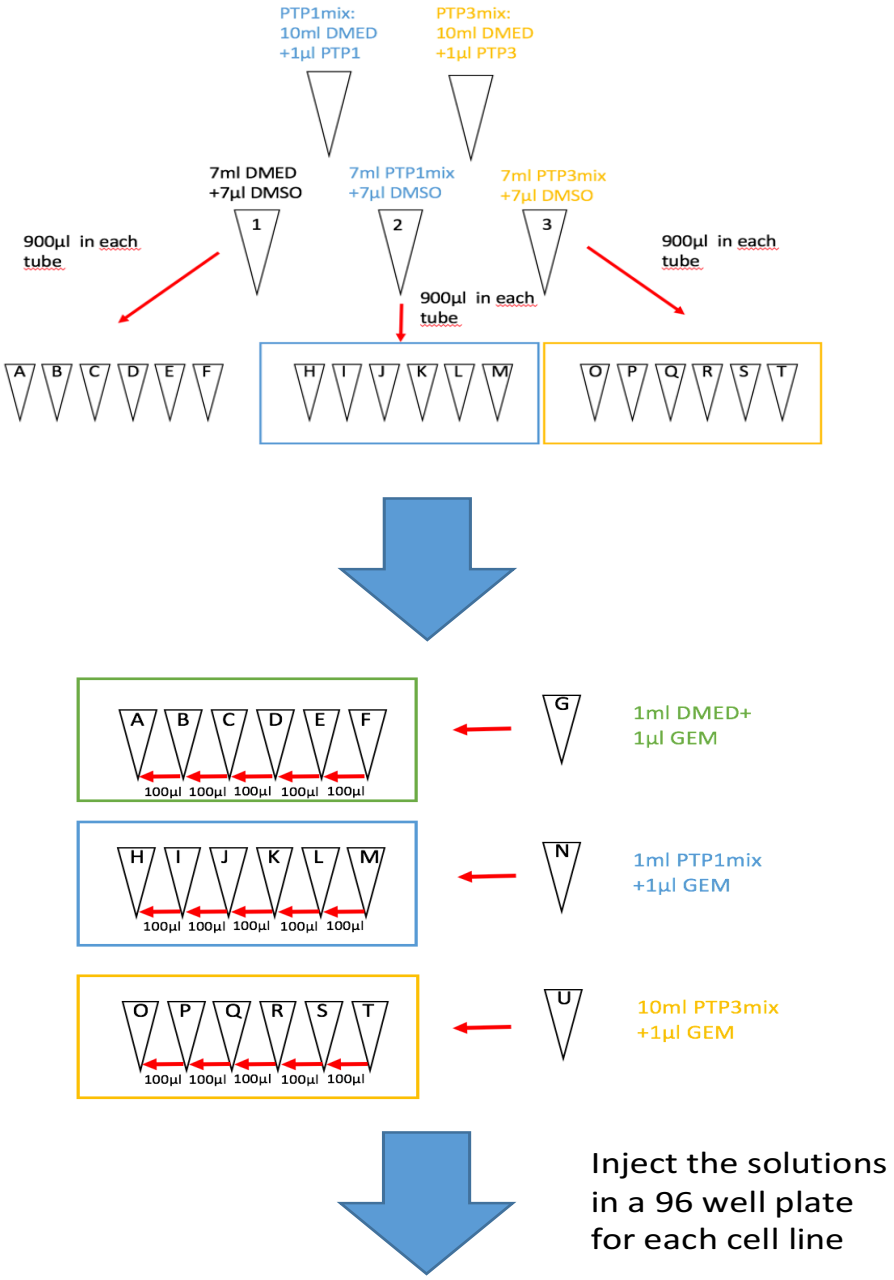

CONCENTRATION OF GEM	GEM/DMSO				GEM/PTP1				GEM/PTP3			
0	1	1	1	1	2	2	2	2	3	3	3	3
100pM	A	A	A	A	H	H	H	H	O	O	O	O
1nM	B	B	B	B	I	I	I	I	P	P	P	P
10nM	C	C	C	C	J	J	J	J	Q	Q	Q	Q
100nM	D	D	D	D	K	K	K	K	R	R	R	R
1uM	E	E	E	E	L	L	L	L	S	S	S	S
10uM	F	F	F	F	M	M	M	M	T	T	T	T
100uM	G	G	G	G	N	N	N	N	U	U	U	U

Figure 7: First treatment scheme used for the cytotoxicity assay.

Altogether, we used three different treatment schemes, in which we treated the cells with the PTPs alone or in combination with GEM, 5FU and PTX. Figure 7 shows one scheme.

Subsequently, cells were incubated for 72 hours.

For the evaluation, the cells were fixed and stained. For the fixation the plates were kept on ice. After aspirating the medium, they were rinsed two times with cold 1xPBS. Afterwards the wells were filled with ice cold 100% methanol and incubated for 10min. The next step was to aspirate or pour out the fixative and move the plates off the ice to room temperature. The wells were then filled with a 0,5% crystal violet solution in 25% methanol. 10 min later, crystal violet was removed (can be filtered and reused). The plates were washed with desalted water until the dye stopped coming off. They were dried at room temperature. The last step was adding 100µl of a 1% SDS (sodium dodecyl sulfate) solution in each well and wait for the crystal violet to dissolve, for that the plates were placed on a shaking plate.

3.4.2 Test evaluation

A difference in the intensity of the colour according to the concentrations of the test substances was already visible to the naked eye. The intensity of the colouring was measured using a microplate-reader (TECAN Infinite® 200 PRO) where the absorbance at a wavelength of 595nm was measured. The result was displayed in an Excel sheet. The average as well as the average relative to DMSO-treated cells was calculated and shown in a diagram. The classical T-Test and Anova were used to evaluate the synergistic effects of the PTPs with GEM, 5FU and PTX.

3.5 Apoptosis quantitative detection and cell cycle analysis

3.5.1 Principle of FACS [15]

Flow cytometry is a laser-based technology, widely used to analyze the expression of cell surface and intracellular molecules. It is also helpful for characterizing and

defining different cell types in heterogeneous cell populations. It can assess the purity of isolated subpopulations, as well as analyze cell size and volume.
Flow cytometry mostly measures the intensity of fluorescence produced by fluorescence-marked antibodies detecting proteins or ligands binding to a specific cell-associated molecule, for instance propidium iodide binding to DNA.

The fluidic system [15]

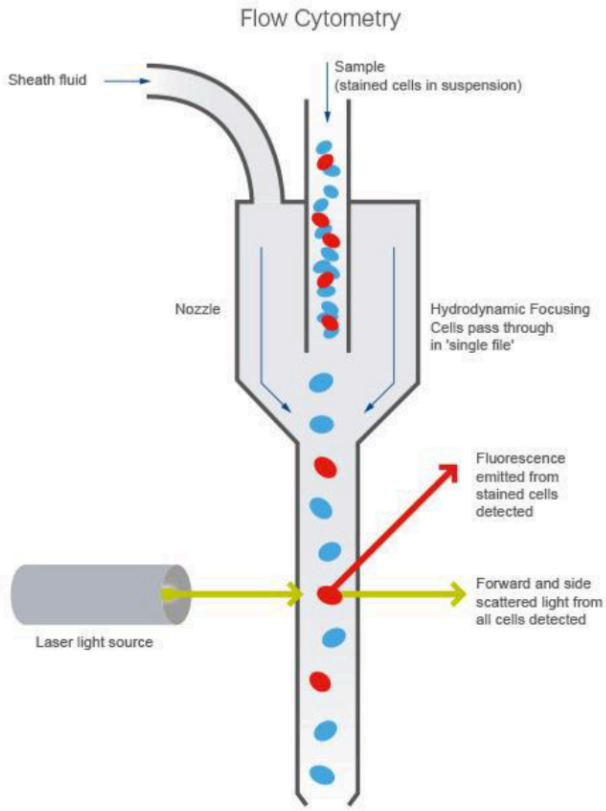

Figure 8: Sheath fluids focus the cell suspension. Cells pass through a laser beam one cell at a time. Forward and side scatter lights, as well as fluorescence signals are detected and recorded.

When the cell suspension runs through the cytometer, it is focused using sheath fluids. The fluid presses the cell suspension hydrodynamically through a very small nozzle. The cells pass the laser lights one cell at a time (Figure 8).
The light that is scattered from cells or particles is detected as they pass through the laser. Detectors in front of the light measure the forward scatter (FS), detectors to the side measure side scatter (SS), fluorescence detectors measure the emitted fluorescence of positively stained cells or particles.

The measurement of forward and side scatter of light and fluorescence [15]

Cells and particles passing the beam scatter light, will be detected as FS and SS. The FS gives information about the size of the cell and the SS is proportional to the cell granularity. With these two parameters cell populations can already be distinguished.

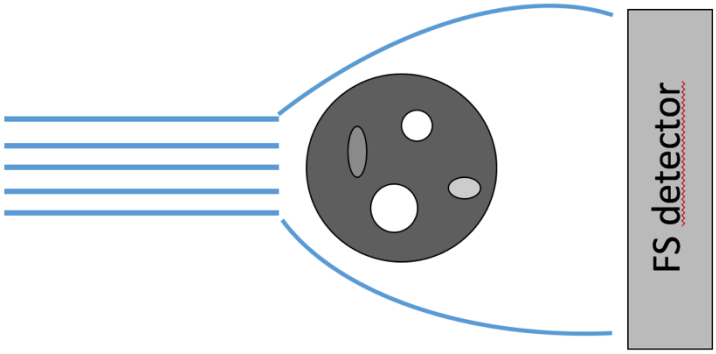

Figure 10: Principle of FS detector. Laser light is diffracted around the cell. The cell size correlates with forward scattered light.

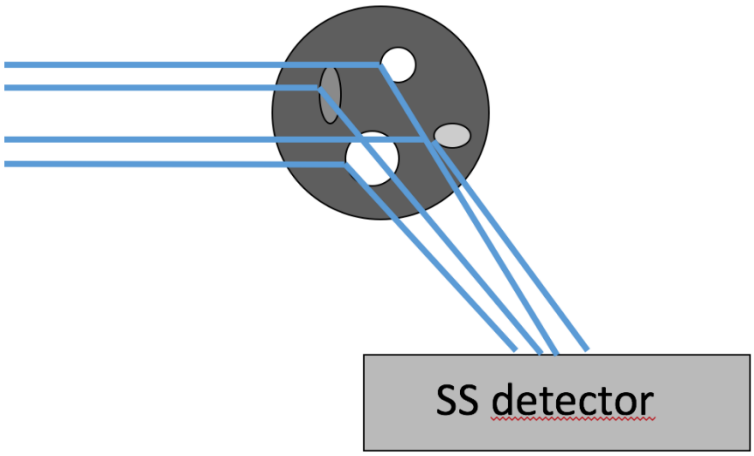

Figure 9: Principle of SC detector. Laser beams are scattered in/on the cell. The intensity of the scattered light correlates with the granularity of the cell.

Not only can cells be separated based on FS and SS, but also by the expression of certain proteins. These proteins are stained with fluorochromes, which emit light when excited by a laser with the corresponding wavelength. These stained cells can be detected individually.

In the flow cytometer the fluorescent light is filtered with sensors. Each sensor will only detect fluorescence at a specified wavelength. The sensors are called

photomultiplying tubes (PMTs). The PMTs convert the energy of a photon into an electric signal.

Also various filters are used to direct photons of the correct wavelength to each PMT. A band pass filter allows transmission of photons with wavelengths within a certain range, short pass (SP) filters allow transmission below a specified wavelength and long pass (LP) filters allow the transmission above a specified wavelength. There are also dichroic mirrors/filters, such as LP dichroic mirrors, which are positioned at a 45° angle to the light beam. A LP dichroic filter photons above a specific wavelength, which are transmitted, and photons below the specific wavelength, which are reflected at a 90° angle.

Every time a fluorescing cell passes the laser beam, a peak or a pulse of photon emission over time is created. The PMT converts it to a voltage pulse, also known as an event.

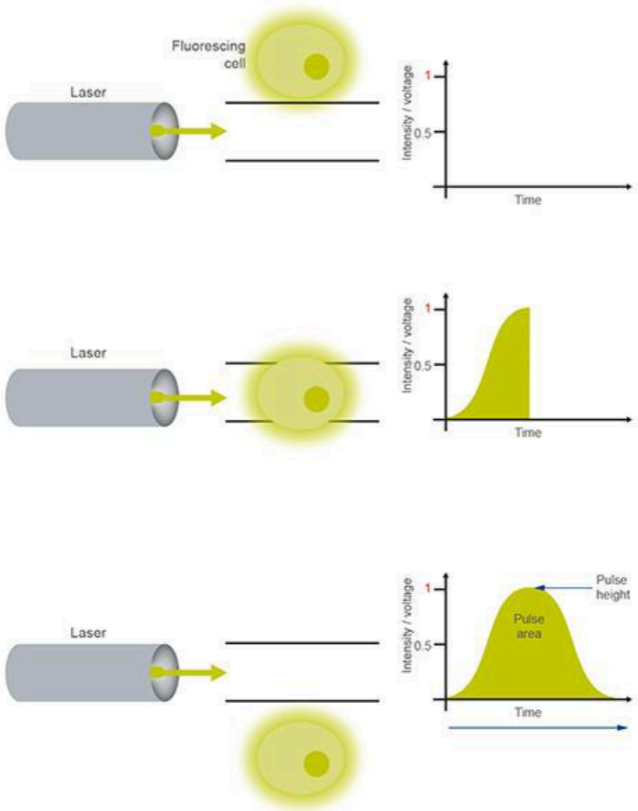

Figure 11: When the fluorescent labeled cell passes through and is interrogated by the laser, photons are emitted. Each time a fluorescing cell releases a photon the PMT measures the pulse area of the voltage. Every time a cell completes its path through the laser beam, it leaves a pulse of voltage over time.

Quantitative detection of apoptosis [16]

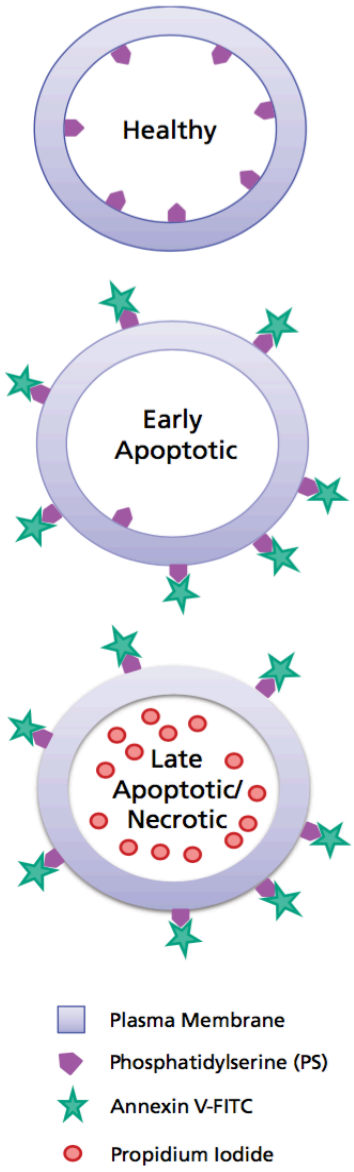

Figure 12: Healthy and apoptotic cells with markers for detection of apoptosis

The programmed cell death, also called apoptosis, is a physiological process for the removal of unwanted cells. It is characterized by a lot of morphological features, one of them is the loss plasma asymmetry and attachment, which happens at the very beginning of this process. During apoptosis the membrane phospholipid phosphatidylserine (PS) is translocated from the inner to the outer side of the plasma membrane. Annexin V is a Ca^{2+}-dependent phospholipid-binding protein with high affinity for PS. It binds only to exposed apoptotic cell surface PS. Annexin V not only stains the apoptotic cells but also the necrotic cells, because their membranes are not intact anymore, therefore the PS in the inside of the membrane is also stained. To distinguish between early and late apoptotic cells staining wit Annexin V is often conjugated with a vital dye such as propidium iodide (PI). Viable cells with intact membranes are not permeable for PI. Therefore, viable cells are both Annexin V and PI negative, early apoptotic cells are Annexin V positive and PI negative and late apoptotic or dead cells are Annexin V and PI positive (Figure 12).

Cell cycle analysis [17]

There are several widely used procedures to analyze the cell cycle. The method we used was based on staining cellular DNA with PI. Through this method, the distribution of cells in the three major phases of the cell cycle (G0/G1 vs. S vs. G2/M) can be detected.

This is because cells in the S phase have more DNA than cells in G1. Cells in the S phase take up more dye and are brighter. The cells in G2 will be approximately twice as bright as cells in G1 because they have double DNA content.

3.5.2 Procedure

PatuS cells were harvested, counted and seeded in a 6cm dish at a density of $2x10^6$ cells/dish, PANC1 cells were seeded at a density of $1x10^6$ cells/dish. Twenty-four hours later the medium was replaced with 2ml of fresh medium containing the test substances in the desired concentrations.
For each experiment and each cell line 5 dishes were seeded, one containing 100 µM DMSO (as a control), one with 10µM PTP1, one with 100µM PTP1, one with 10µM PTP3 and one with 100µM PTP3. Subsequently, the cells were incubated for 24, 48 and 72 hours.

For the detection of **apoptosis** the supernatant must be kept. After washing two times with PBS, 1ml trypsin-EDTA solution was added. The cells were incubated until they detached. The enzymatic reaction was stopped with the supernatant. The cells were centrifuged at 1200rmp for 5min at room temperature and the medium was aspirated. The cells were washed with cold cell staining buffer (PBS + 5% FBS). After resuspending the cells in 1ml Annexin V binding buffer, the cells were counted and diluted in Annexin V binding buffer to a concentration of $1x10^6$ cells/ml. Annexin V binding buffer is a solution of 500µl HEPES (1M), 125µl $CaCl_2$ (1M), 14000µl NaCl (5M) and water filled up to 50ml. 50µl of the cell suspension were transferred into a 5ml test tube. 5µl Annexin V and 10µl PI of a 50µg/ml stock solution of PI in 1x PBS were added. After vortexing, the cells were incubated for 15min at room temperature and in the dark. 400µl of Annexin V binding buffer were pipetted into the solution and the fluorescence was measured within an hour.

For analyzing the **cell cycle** the cells were harvested through trypsinization as described. After centrifugation (1200rpm, 5min, room temperature) the cells were washed in PBS and again centrifuged. PBS was aspirated and the pellets were kept on ice. For the fixation cold ethanol (70%) was used. Ethanol was added drop wise to the cell pellet while vortexing. The fixed cells were kept at 4°C until the

analysis. For this, the cells were centrifuged at 850g for 5min and ethanol was aspirated. Again the cells were washed two times in PBS. To make sure that only DNA will be stained and not RNA, the cells were treated with 50µl ribonuclease (RNAse) before 200µl PI stock solution were added.

3.5.3 Imaging cells

Before harvesting the cells, pictures were taken with a microscope (Nikon Eclipse-Ti), to follow morphological changes.

All the samples from apoptosis and cell cycle experiments were analyzed using a BD flow cytometer. The apoptosis quantity was defined as the sum of the Q2 quadrant.

3.6 Gene expression analysis

3.6.1 RNA extraction

The following figure shows the systematic workflow, which is necessary to perform the gene expression analysis with qPCR.

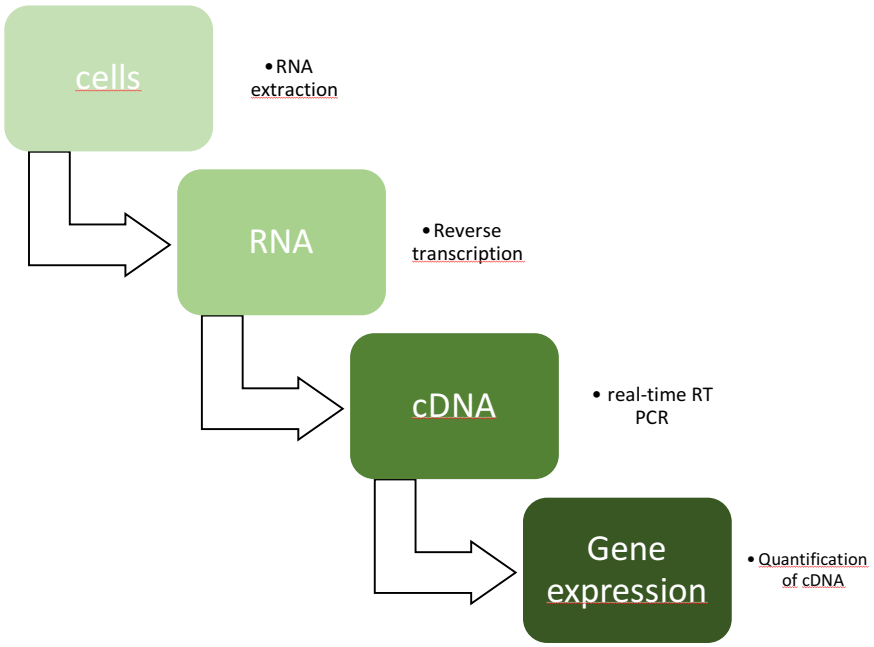

Figure 13: Overview: Sample processing for gene expression analysis.

RNA extraction was performed with Trifast ™ from peqlab following the manufacturer's protocol. RNA was kept at -80°C.

3.6.2 Reverse transcription

Since mRNA is very unstable, it is necessary to convert it into more stable copy-DNA (cDNA) using the mechanism of reverse transcription. For this the RevertAid Reverse Transcriptase (Thermo Fisher Scientific, Austria) was used. After thawing, the RNA was mixed, gently centrifuged and kept on ice. 1µg of total RNA from each sample was pipetted into a sterile, nuclease-free tube on ice. 1µl of random hexamer (0,2µg) was used as a primer, afterwards the sample was filled up with DEPC-treated water to 12,5µl. The tubes were gently mixed and centrifuged. Following components were added in the indicated order (volume for one reaction).

- 5x Reaction Buffer (4µl)
- Thermo Scientific RiboLock RNase Inhibitor (0,5µl)
- dNTP Mix, 10nM each (2µl)
- RevertAid Reverse Transcriptase (1µl)

The samples were incubated in a PCR cycler 10min at 25°C, followed by 60min at 42°C. To terminate the reaction, they were heated at 70°C for 10min. 80µl of nuclease-free water were added to have a final concentration of 10ng/ µl. The samples were stored at -20°C.

3.6.3 Real time reverse transcription polymerase chain reaction

The gene expression analysis was performed with a CFX Connect™ Real-Time PCR Detection System (Bio Rad). The RT-qPCR was performed as a two step assay. In quantitative PCR (qPCR) real-time fluorescence is used to measure the quantity of DNA present at each cycle during PCR.
Both cell lines were analyzed for the gene coding for the NKCC1-cotranporter, which is called SLC12A2.
As a reference, the housekeeping gene Hypoxanthine Phosphoribosyltransferase 1 (HPRT) was used. Primer mixes were prepared beforehand at a final concentration of 10 µM. Before pipetting into the wells, 0,6µl of primer mix was

mixed with 5µl SYBR 2x master mix and 2,4µl nuclease-free water (volumes for one reaction). 2µl of cDNA were added to the each well.
In each cycle the DNA is doubled, which leads to an exponential amplification. SYBR 2x master mix was used as a dye which fluoresces when it is binding to double stranded DNA: After each cycle the fluorescence is measured and represents the amount of copied DNA. Every sample was tested in duplicates, with normalization to the housekeeping gene as an internal control.

3.6.4 Calculation of the gene expression

After measuring the intensity of the fluorescence, the quantity of expressed genes was presented in an Excel sheet as Ct or Cq, which indicates the cycle at which the fluorescence was detected above a minimum threshold.
For each cell line, the mean of the Ct was calculated. From the mean value, the Ct of HPRT was then subtracted to obtain the “delta Ct” or DCt. The expression of SLC12A2 relative to HPRT was then calculated with the following formula: 2^{-DCt}.
The results obtained were presented in a diagram.

3.6.5 Primers for NKCC1

Assay	**Sequence to analyze**
SLC12A2 forward	AGAAGCTGCTCCGGCCTA
SLC12A2 reverse	CACAGCATCTCTGGTTGGAG

3.7 Statistical analysis

All statistical analyzes of this thesis were performed with Excel. P-values <0.05 are considered statistically significant.
For all group comparisons, the t-test for dependent samples and the analysis of variance (ANOVA) were used.

4 RESULTS

This chapter presents the results of the experimental work conducted during this thesis. Details concerning the workflow and the protocols can be found in the sections “Materials and methods”. In addition, the same chapter explains the different procedures applied for the analysis of data and statistical methods in detail.

4.1 Gene expression

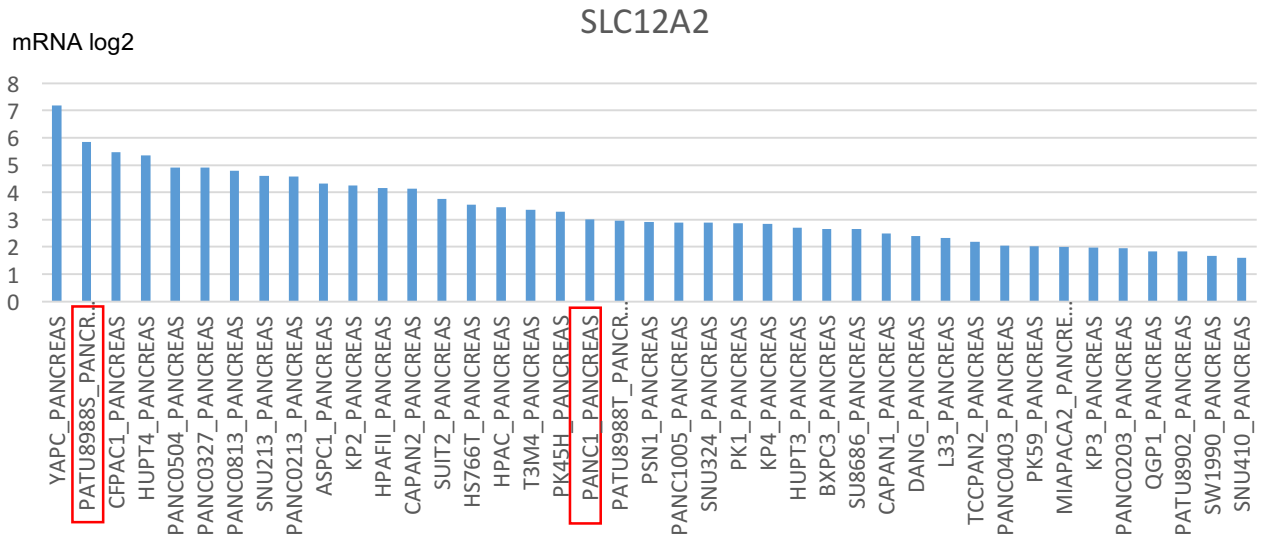

Figure 14: Expression of SLC12A2 in various pancreatic cancer cell lines.

The cell lines PANC1 and PatuS were selected based on the expression of SLC12A2 as reported by the Cancer Cell Line Encyclopedia (CCLE) and shown in Figure 14[18]. Both PatuS and PANC1 express the gene SLC12A2, PatuS having a significantly higher expression. This was

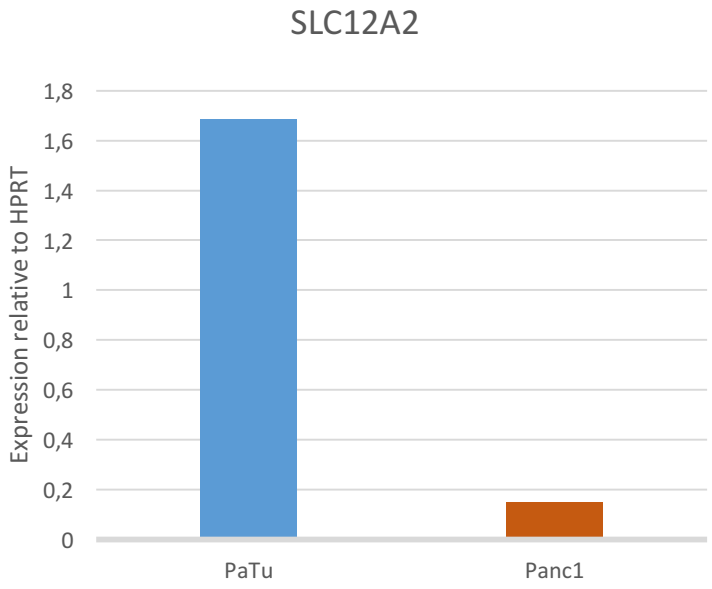

Figure 15: Expression of SLC12A2 in PANC1 and PatuS

confirmed by RT-qPCR (Figure15).

Based on the knowledge that both cell lines express the gene SLC12A2, which encodes for the NKCC1 protein, but that the levels are significantly different, the following studies were limited to these two cell lines as examples of NKCC1-high and NKCC1-low cells.

4.2 Effects of PTPs

In order to detect an effect of the bumetanide derivatives on the cells, cells were treated with increasing concentrations of the three compounds. Gemcitabine was used as control for PaTuS cells, also in increasing concentrations.

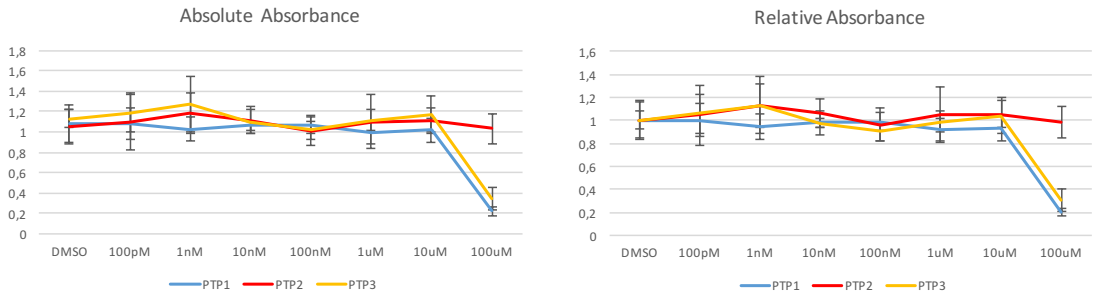

Figure 16: Absolute and relative absorbance measured after treating PANC1 with the derivates.

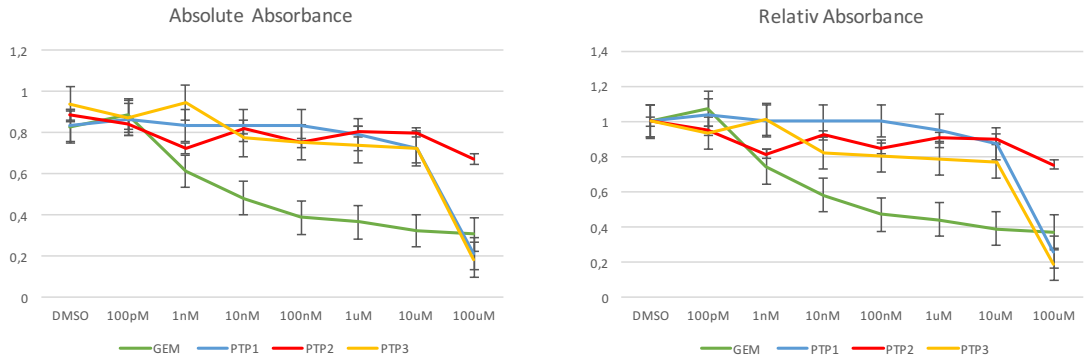

Figure 17: Absolute and relative absorbance measured after treating PatuS with the derivates.

After the cytotoxicity assays (see methods section) the growth of both cell lines was reduced by PTP1 as well as PTP3 at high doses. Furthermore, PatuS reduction in growth was stronger than PANC1, as expected, since the expression of NKCC1-cotransporters in PatuS cells is much higher than in PANC1.
Both cell lines were significant inhibited in growth at a concentration of 10 µM.

PTP2, on the contrary, had no effect in PatuS or in PANC1 and was therefore excluded from further studies (Figures 16 and 17).

4.3 Results of the combination treatments

Since the derivatives showed only a moderate effect, a new strategy was pursued. A popular approach nowadays is based on combinations of different drugs to produce a synergistic effect.
Therefore, the PTPs were mixed in various concentrations with 100nM gemcitabine or 10nM paclitaxel, which are the most commonly used drugs in pancreatic cancer.
For this purpose, the cells were incubated with different mixes of PTPs, GEM and PTX for 72 hours.

4.3.1 PANC1 and PatuS with PTP1+GEM and PTP3+GEM

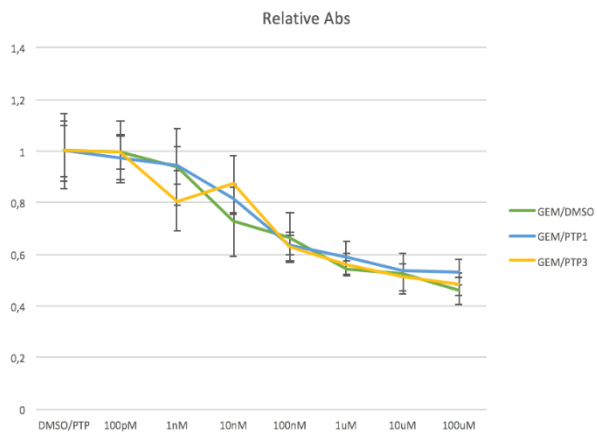

Figure 18: Relative absorbance of PANC1 after treating with mixes of GEM combined with various concentrations of PTP1 and PTP3 (0, 100pM, 1nM, 10nM, 100nM, 1uM, 10uM, 100uM). 5000 cells/well were used, 3 experiments each with 3 96 well plates for 72hours.

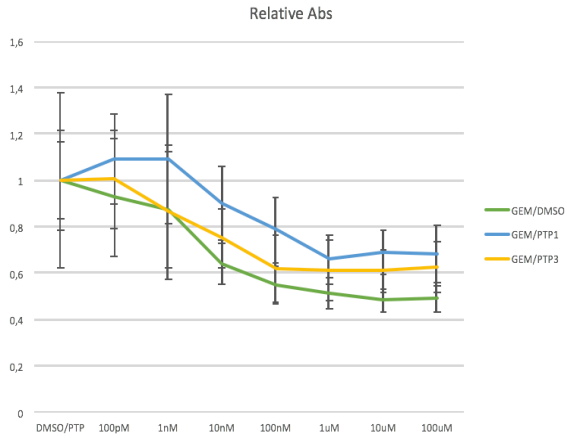

Figure 19: Relative absorbance of PatuS after treating with mixes of GEM combined with various concentrations of PTP1 and PTP3 (0, 100pM, 1nM, 10nM, 100nM, 1uM, 10uM, 100uM). 5000 cells/well were used, 3 experiments each with 3 96 well plates for 72hours.

In both cell lines, treatment with PTP1 or PTP3 at concentrations ranging from 100pM to 100µM did not have any synergistic or additive effect over GEM alone (Figures 18 and 19).

4.3.2 PANC1 and PatuS with PTP1+PTX and PTP3+PTX

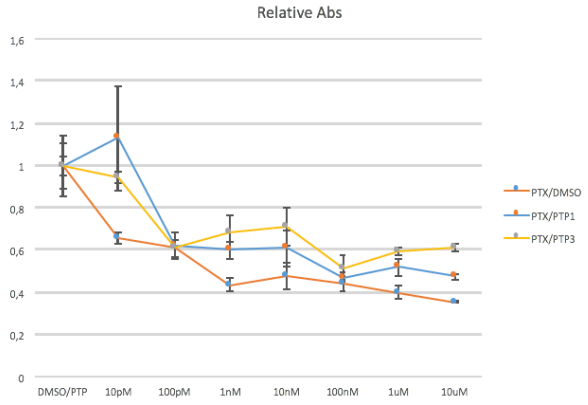

Figure 20: Relative absorbance of PANC1 after treating with mixes of PTX combined with various concentrations of PTP1 and PTP3 (0, 10pM, 100pM, 1nM, 10nM, 100nM, 1uM, 10uM). 5000 cells/well were used, three experiments each with three 96 well plates for 72hours

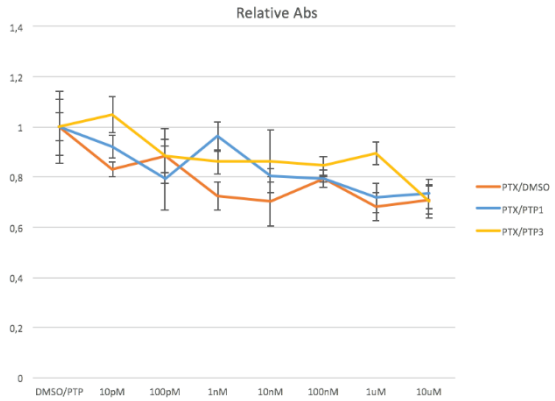

Figure 21: Relative absorbance of PatuS after treating with mixes of PTX combined with various concentrations of PTP1 and PTP3 (0, 10pM, 100pM, 1nM, 10nM, 100nM, 1uM, 10uM). 5000 cells/well were used, three experiments each with three 96 well plates for 72h.

The combination of PTPs with PTX gave more complex results (Figures 20 and 21).

The dose-response curves showed some differences here. In PANC1, PTX alone at a concentration of 10pM showed already a growth inhibitory effect, whereas the combination with PTP1 and PTP3 did not appear to be effective at the same concentration, suggesting some inhibitory effect (Figure 20). Higher doses of PTP1 or PTP3 partially reverted this. PatuS cells were in general not very sensitive to PTX or the combinations (Figure 21).

4.3.3 PANC1 and PatuS with PTP1+GEM, PTP1+PTX and PTP1+5FU

In order to operate the study more effectively, a new scheme was developed, making it possible to gather more information at the same time. In this new setting, three doses of PTP1 or PTP3 were combined with 3 doses of GEM, PTX, or 5FU, to analyze more conditions (Figures 22-27).

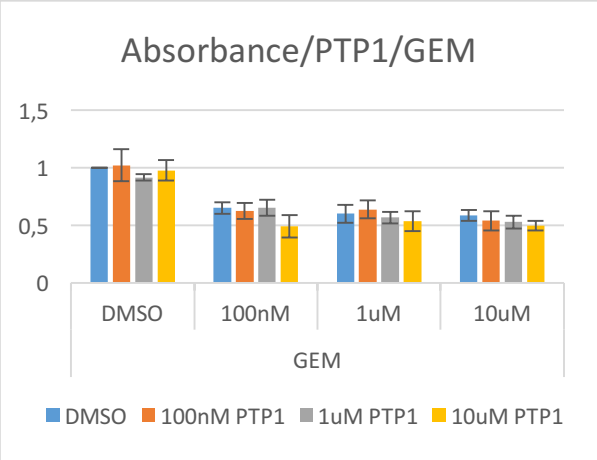

Figure 24 Relative absorption of PANC1 after treatment with various concentrations of GEM and PTP1. 5000 cells/ well, four experiments with four 96 well plates each for 72h.

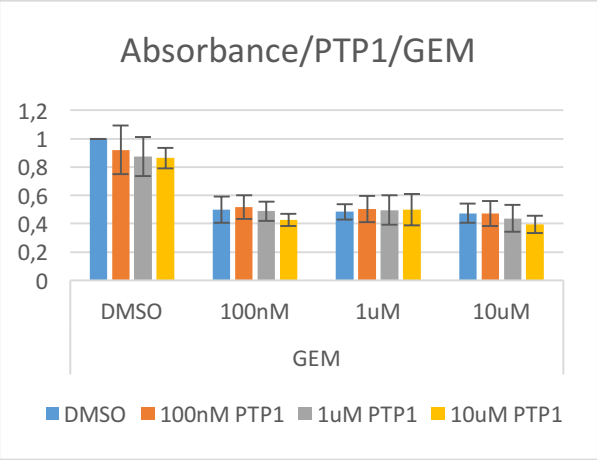

Figure 25: Relative absorption of PatuS after treatment with various concentrations of GEM and PTP1. 20000 cells/well, three experiments with three 96 well plates each for 72h.

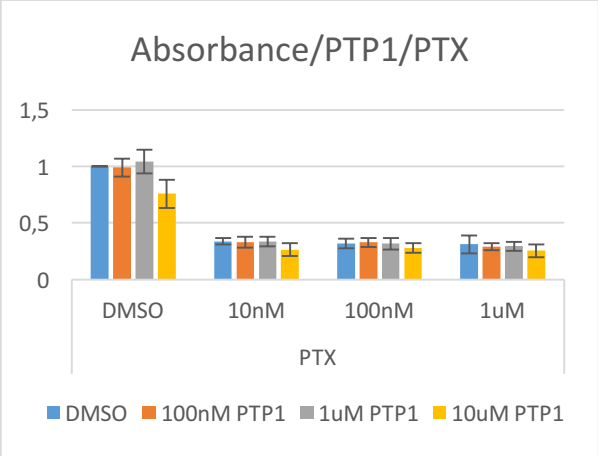

Figure 22: Relative absorption of PANC1 after treatment with various concentrations of PTX and PTP1. 5000 cells/well, four experiments with four 96 well plates each for 72h.

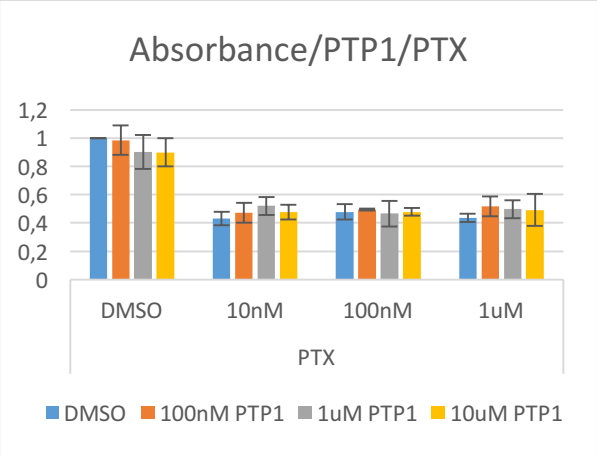

Figure 23: Relative absorption of PatuS after treatment with various concentrations of PTX and PTP1. 20000 cells/well, three experiments with three 96 well plates each for 72h.

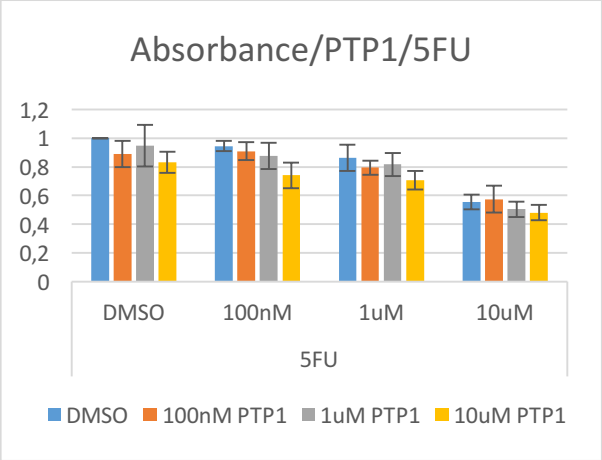

Figure 27: Relative absorption of PANC1 after treatment with various concentrations of 5FU and PTP1. 5000 cells/well, four experiments with four 96 well plates each for 72h.

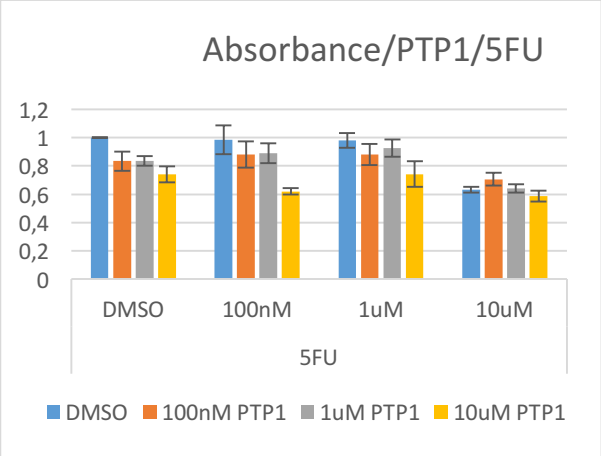

Figure 26: Relative absorption of PatuS after treatment with various concentrations of 5FU and PTP1. 20000 cells/well, three experiments with three 96 well plates each for 72h.

5FU, like GEM and PTX, is one of the most commonly used drugs in pancreatic cancer.

In these conditions, we confirmed that GEM, PTX, and, to a lesser extent, 5FU reduce the growth of PANC1 and PaTuS cells, as shown in figures 18-21, while PTP1 did not have a prominent additive effect in any condition.

PTP1 alone was not that as effective at reducing cell growth as in combination with the drugs (GEM, PTX and 5FU). Especially the combinations with GEM ad PTX showed a significant effect in contrast to PTP1 with DMSO.
5FU had less impact on the effect. The inhibition of cell growth increased only slowly with increasing concentration of 5FU.

4.3.4 PANC1 and PatuS with PTP3+GEM, PTP3+PTX and PTP3+5FU

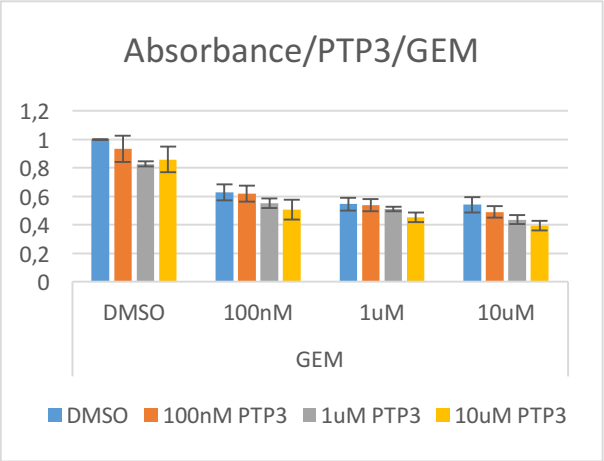

Figure 28: Relative absorbance of PANC1 after treatment with various concentrations of GEM and PTP3. 5000 cells/well, four experiments with four 96 well plates each for 72h.

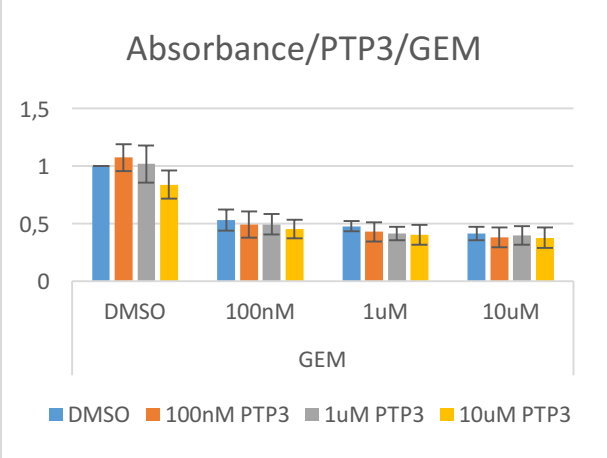

Figure 29: Relative absorbance of PatuS after treatment with various concentrations of GEM and PTP3. 20000 cells/well, three experiments with three 96 well plates each for 72h.

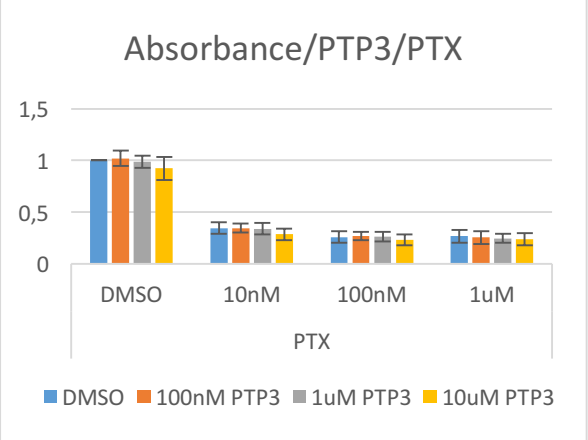

Figure30: Relative absorbance of PANC1 after treatment with various concentrations of PTX and PTP1. 5000 cells/well, four experiments with four 96 well plates each for 72h.

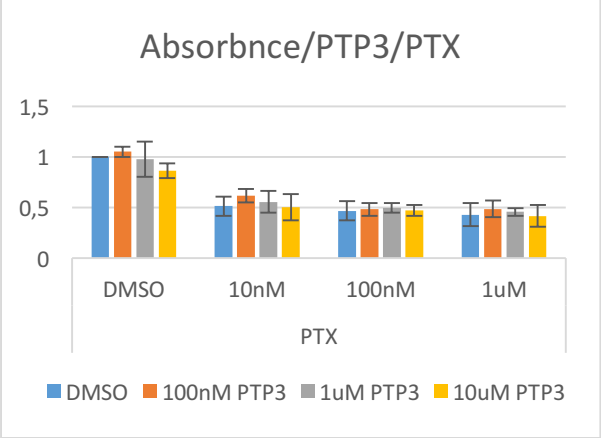

Figure 31: Relative absorbance of PatuS after treatment with various concentrations of PTX and PTP3. 20000 cells/well, three experiments with three 96 well plates each for 72h.

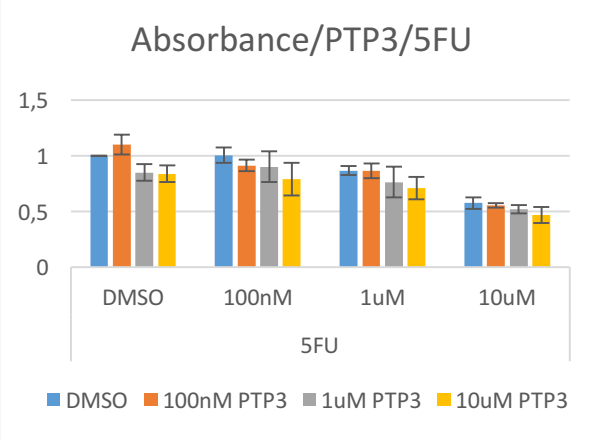

Figure 32: Relative absorbance of PANC1 after treatment with various concentrations of 5FU and PTP3. 5000 cells/ well, four experiments with four 96 well plates each for 72h.

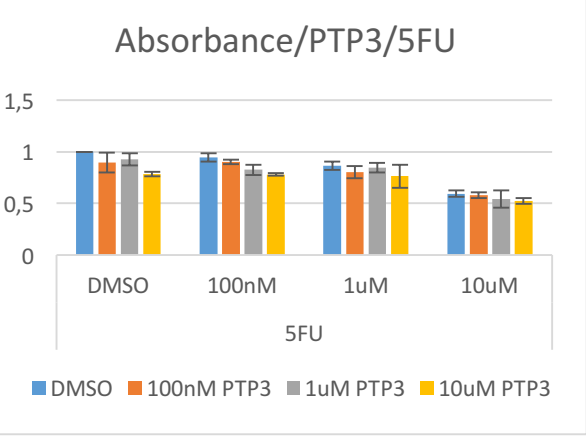

Figure 33: Relative absorbance of PatuS after treatment with various concentrations of 5FU and PTP3. 20000 cells/well, three experiments with three 96 well plates each for 72h.

Similar results were observed when combining chemotherapeutic agents with PTP3 (Figures 28-33). The combination of different doses of PTP3 did not improve the cytostatic/cytotoxic effects of any of the chemotherapeutic agents at the tested concentrations. Only in the combination with GEM at a concentration of 10uM, a small additive effect was observed in PANC1 cells.

To test whether this effect occurred by chance, the paired student t-test and a one-way ANOVA analysis of variance were performed on four biological replicates.

T-TEST

Plate	DMSO	100nM PTP3	1uM PTP3	10uM PTP3
1	0,594807664	0,453334407	0,402012275	0,403121302
2	0,558027652	0,551407271	0,46291876	0,440706165
3	0,469053011	0,480518156	0,460616405	0,363525309
4	0,54348668	0,477189836	0,416582609	0,372410585

Table 1: Measured Absorbance of PANC1 with GEM (10uM) and increasing concentrations of PTP3 (0, 100nM, 1uM, 10uM).

	DMSO	*100nM PTP3*
Mean	0,541343752	0,490612418
Variance	0,002789095	0,001789241
Observations	4	4
Pooled Variance	0,002289168	
Hypothesized Mean Difference	0	
df	6	
t Stat	1,499520542	
P(T<=t) one-tail	0,092200585	
t Critical one-tail	1,943180281	
P(T<=t) two-tail	0,18440117	
t Critical two-tail	2,446911851	

Table 2: T-Test (Two-Sample Assuming Equal Variances) between two dependent samples (DMSO and 100nM).

	DMSO	*1uM PTP3*
Mean	0,541343752	0,435532512
Variance	0,002789095	0,000953971
Observations	4	4
Pooled Variance	0,001871533	
Hypothesized Mean Difference	0	
df	6	
t Stat	3,458979861	
P(T<=t) one-tail	0,006742044	
t Critical one-tail	1,943180281	
P(T<=t) two-tail	0,013484089	
t Critical two-tail	2,446911851	

Table 3: T-Test (Two-Sample Assuming Equal Variances) between two dependent samples (DMSO and 1uM).

	DMSO	*10uM PTP3*
Mean	0,541343752	0,39494084
Variance	0,002789095	0,001218644
Observations	4	4
Pooled Variance	0,00200387	
Hypothesized Mean Difference	0	
df	6	
t Stat	4,625194122	
P(T<=t) one-tail	0,00179787	
t Critical one-tail	1,943180281	
P(T<=t) two-tail	0,003595739	
t Critical two-tail	2,446911851	

Table 4: T-Test (Two-Sample Assuming Equal Variances) between two dependent samples (DMSO and 10uM).

	100nM PTP3	*1uM PTP3*
Mean	0,490612418	0,435532512
Variance	0,001789241	0,000953971
Observations	4	4
Pooled Variance	0,001371606	
Hypothesized Mean Difference	0	
df	6	
t Stat	2,103262393	
P(T<=t) one-tail	0,040057758	
t Critical one-tail	1,943180281	
P(T<=t) two-tail	0,080115517	
t Critical two-tail	2,446911851	

Table 5: T-Test (Two-Sample Assuming Equal Variances) between two dependent samples (100nM and 1uM).

	100nM PTP3	*10uM PTP3*
Mean	0,490612418	0,39494084
Variance	0,001789241	0,001218644
Observations	4	4
Pooled Variance	0,001503943	
Hypothesized Mean Difference	0	
df	6	
t Stat	3,488849775	
P(T<=t) one-tail	0,006500777	
t Critical one-tail	1,943180281	
P(T<=t) two-tail	0,013001555	
t Critical two-tail	2,446911851	

Table 6: T-Test (Two-Sample Assuming Equal Variances) between two dependent samples (100nM and 10uM).

	1uM PTP3	*10uM PTP3*
Mean	0,435532512	0,39494084
Variance	0,000953971	0,001218644
Observations	4	4
Pooled Variance	0,001086308	
Hypothesized Mean Difference	0	
df	6	
t Stat	1,741708658	
P(T<=t) one-tail	0,066098848	
t Critical one-tail	1,943180281	
P(T<=t) two-tail	0,132197697	
t Critical two-tail	2,446911851	

Table 7: T-Test (Two-Sample Assuming Equal Variances) between two dependent samples (1uM and 10uM).

The p-value describes the probability that the effects observed in a study could have occurred by chance alone (the p-value lies between 0 and 1). The smaller the p-value, the lower the probability that the result can be explained by chance. For this research questions it has been agreed upon to regard a p-value of (or smaller than) 0.05 as “statistically significant” (this corresponds to the probability of a result caused by chance of at most 5%) [19].

The p-value is <0.05 when comparing the means for the group of DMSO with 1uM PTP3, DMSO with 10uM PTP3, 100nM PTP3 with 1uM PTP3 and 100nM PTP3 with 10uM PTP3 and therefore there is a significant difference between these groups (Figure 34).

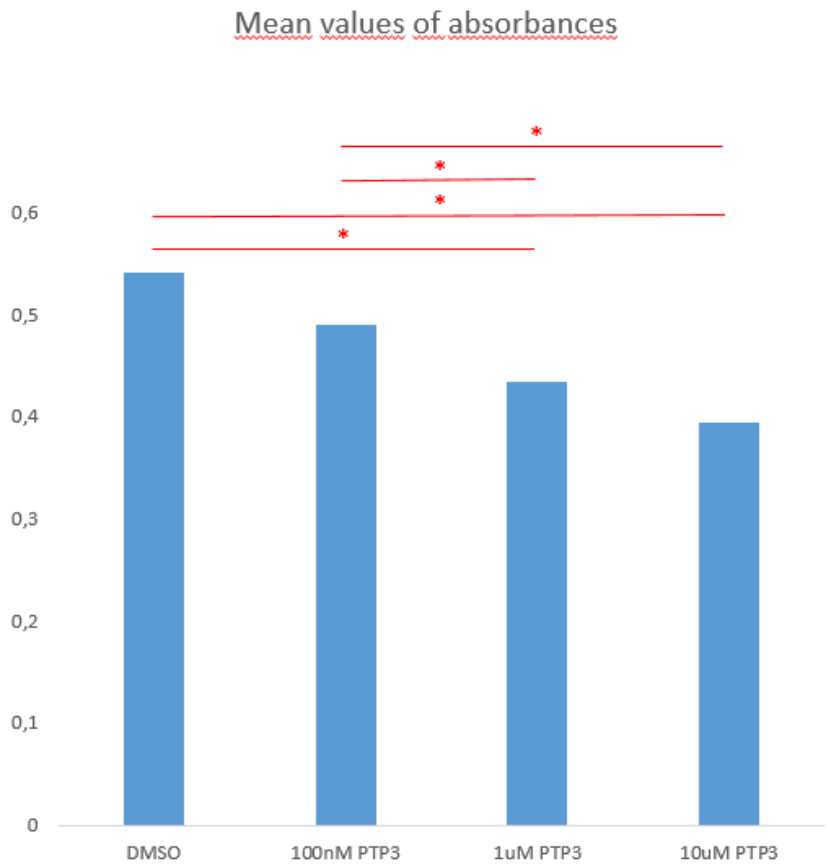

Figure 34: Mean values of PANC1 cells treated with GEM (10uM) and various concentrations of PTP3.

ANOVA

Analysis of variance (ANOVA) is one of the most frequently used statistical methods in medical research. The main interest of analysis is focused on the differences of group means; however, ANOVA focuses on the difference of variances [20].

ANOVA

Source of Variation	*SS*	*df*	*MS*	*F*	*P-value*	*F crit*
Between Groups	0,04903803	3	0,01634601	9,685158404	0,001582596	3,490294819
Within Groups	0,020252856	12	0,001687738			
Total	0,069290886	15				

Table 8: Analysis of variance between all groups.

Also the analysis of variance shows a stastically significanc between these groups, whereby the null hypothesis can be rejected, which states that the differences between the means are based on chance.

4.4 Results of quantitative detection of apoptosis

To detect the amount of apoptotic cells, flow cytometry was used. The gross majority of classical apoptotic hallmarks can be rapidly examined by flow and image cytometry. [21]

Before analyzing the cells, pictures were taken and examined for any morphological changes, using a microscope (Nikon Eclipse-Ti).

4.4.1 PANC1 treated with DMSO, 10uM PTP1, 100uM PTP1, 10uM PTP3 and 100uM PTP3 after **24 hours**

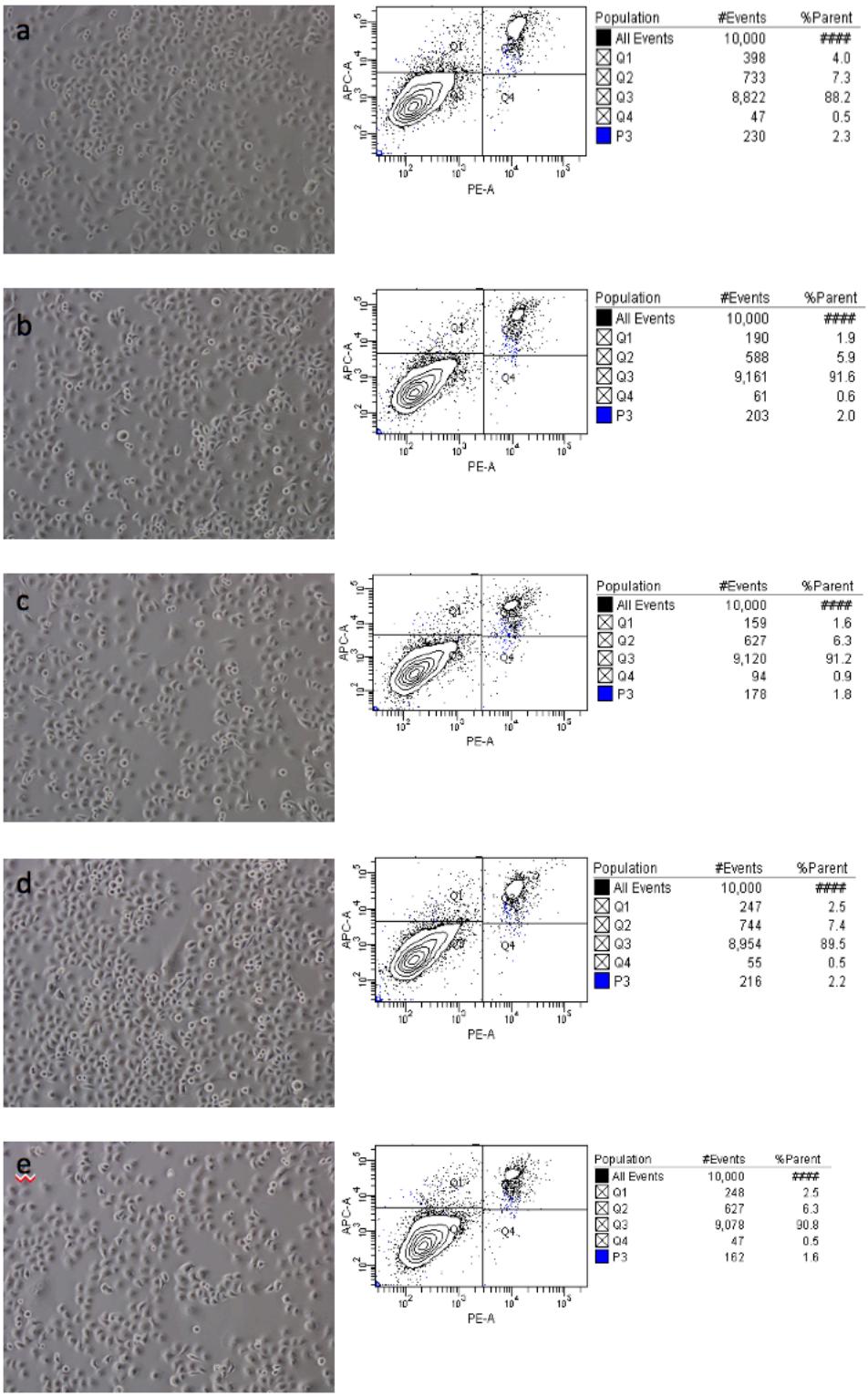

Figure 28a-e:
LEFT: Microscopic picture of PANC1 a. after treating with DMSO for 24h, b. after treating with PTP1 (10uM) for 24h, c. after treating with PTP1 (100uM) for 24h, d. after treating with PTP3 (10uM) for 24h and e. after treating with PTP3 (100uM) for 24h.
RIGHT: Flow cytometry of PANC1 a. after treating with DMSO for 24h, b. after treating with PTP1 (10uM) for 24h, c. after treating with PTP1 (100uM) for 24h, d. after treating with PTP3 (10uM) for 24h. and e. after treating with PTP3 (100uM) for 24h. Cells are stained with Annexin V and PI

After 24 hours treatment with PTP1 (10uM) there was hardly any reduction of the living cells in the microscopic images, which was confirmed by the FACS data.

Also, increasing the concentration of PTP1 from 10uM to 100uM did not make much of a difference.

However, a reduction of the density of living cells can be clearly observed in the Figures 35d and 35e, although an increase of Q2 (%) could not be seen by FACS. This result could have arisen from a faulty handling of the cells, because all controls worked properly.

4.4.2 PANC1 treated with DMSO, 10uM PTP1, 100uM PTP1, 10uM PTP3 and 100uM PTP3 after **48 hours**

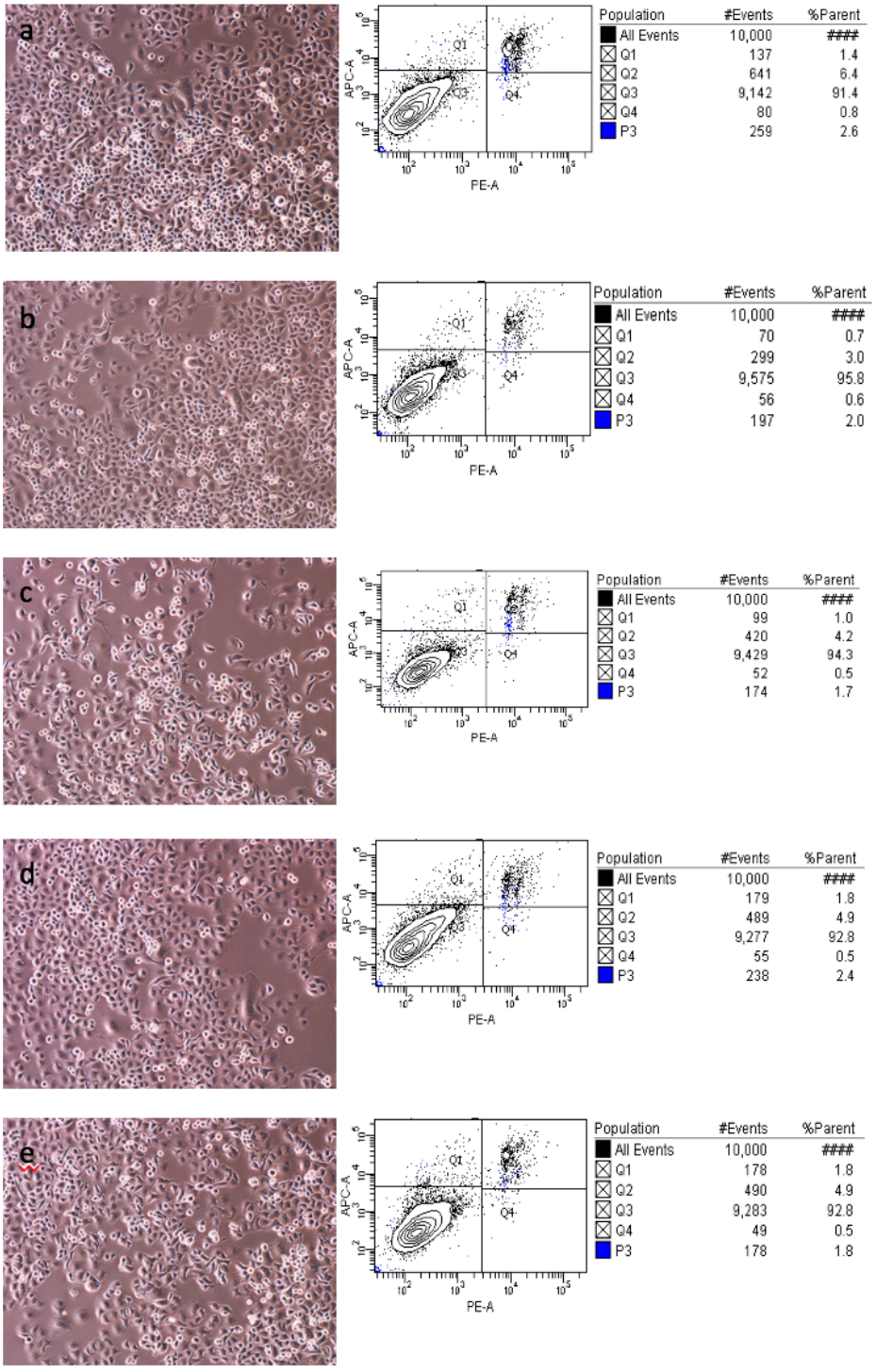

Figure 29a-e:
LEFT: Microscopic picture of PANC1 ***a.*** *after treating with DMSO for 48h,* ***b.*** *after treating with PTP1 (10uM) for 48h,* ***c.*** *after treating with PTP1 (100uM) for 48h,* ***d.*** *after treating with PTP3 (10uM) for 48h and* ***e.*** *after treating with PTP3 (100uM) for 48h. RIGHT: Flow cytometry of PANC1* ***a.*** *after treating with DMSO for 48h,* ***b.*** *after treating with PTP1 (10uM) for 48h,* ***c.*** *after treating with PTP1 (100uM) for 48h,* ***d.*** *after treating with PTP3 (10uM) for 48h. and* ***e.*** *after treating with PTP3 (100uM) for 48h. Cells are stained with Annexin V and PI*

Also after 48 hours, no striking effect was observed in the microscopic images and as well as in the data of FACS.

4.4.3 PANC1 treated with DMSO, 10uM PTP1, 100uM PTP1, 10uM PTP3 and 100uM PTP3 after **72 hours**

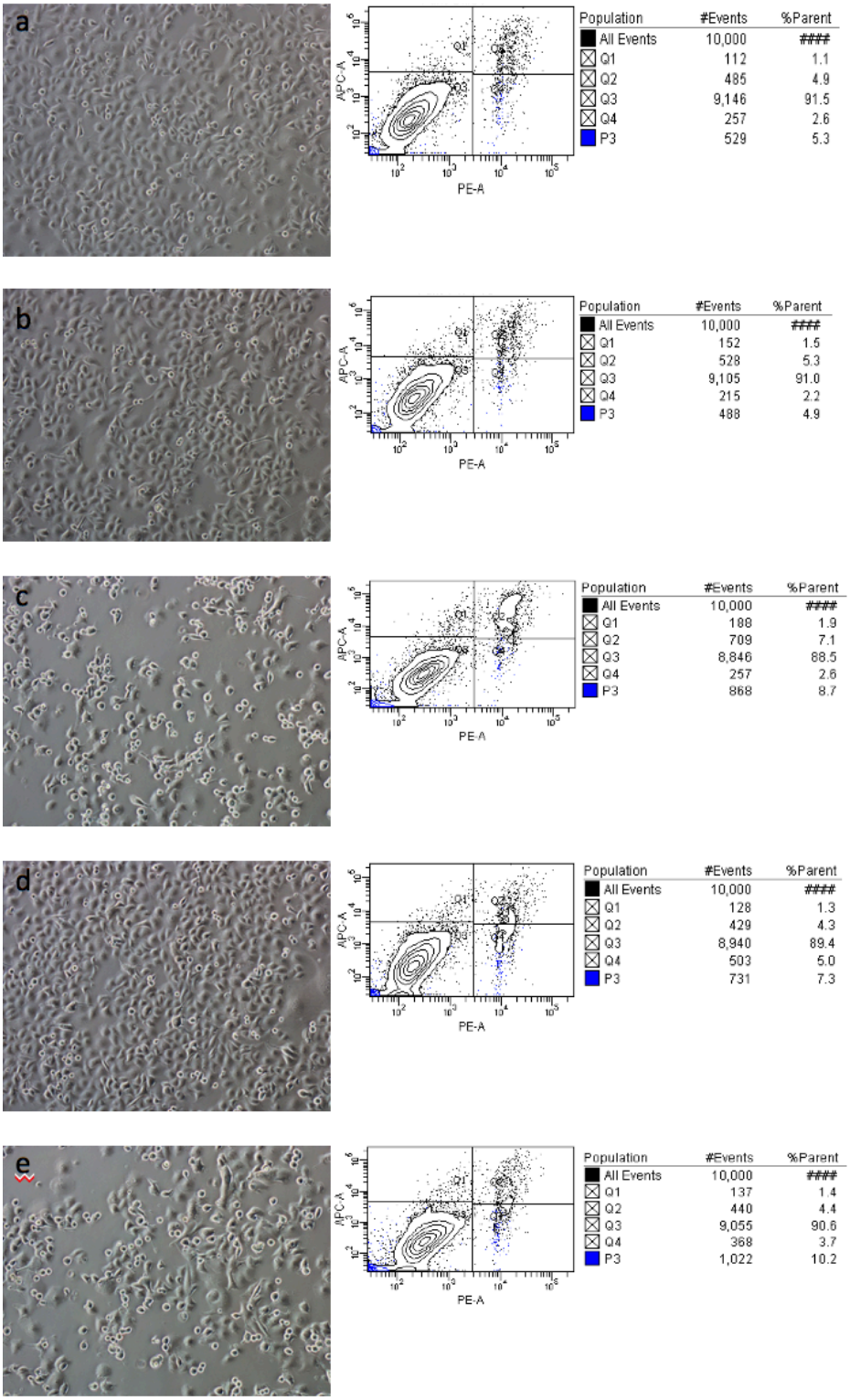

Figure 30a-e:
LEFT: Microscopic picture of PANC1 ***a.*** *after treating with DMSO for 72h,* ***b.*** *after treating with PTP1 (10uM) for 72h,* ***c.*** *after treating with PTP1 (100uM) for 72h,* ***d.*** *after treating with PTP3 (10uM) for 72h and* ***e.*** *after treating with PTP3 (100uM) for 72h. RIGHT: Flow cytometry of PANC1* ***a.*** *after treating with DMSO for 72h,* ***b.*** *after treating with PTP1 (10uM) for 72h,* ***c.*** *after treating with PTP1 (100uM) for 72h,* ***d.*** *after treating with PTP3 (10uM) for 72h. and* ***e.*** *after treating with PTP3 (100uM) for 72h. Cells are stained with Annexin V and PI.*

The results after 72 hours looked more promising.

The bumetanide derivatives had little effect at a concentration of 10uM. However, with a concentration of 100uM of both PTP1 and PTP3, an increase in the Q2 value was observed, which was also confirmed in the microscopic images.

4.4.4 PatuS with DMSO, 10uM PTP1, 100uM PTP1, 10uM PTP3 and 100uM PTP3 after **24 hours**

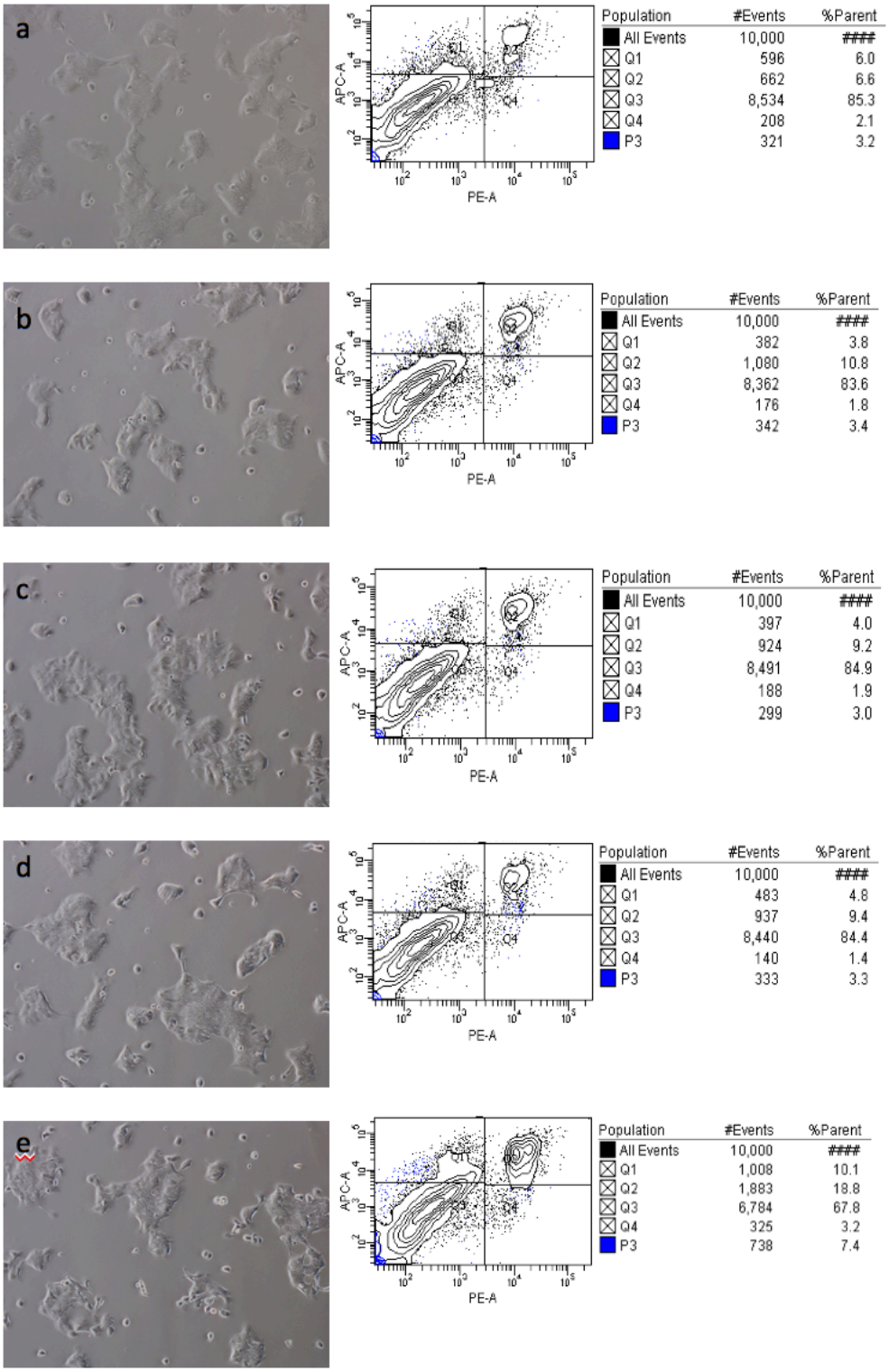

Figure 31a-e:
*LEFT: Microscopic picture of PatuS **a.** after treating with DMSO for 24h, **b.** after treating with PTP1 (10uM) for 24h, **c.** after treating with PTP1 (100uM) for 24h, **d.** after treating with PTP3 (10uM) for 24h and **e.** after treating with PTP3 (100uM) for 24h.*
*RIGHT: Flow cytometry of PatuS **a.** after treating with DMSO for 24h, **b.** after treating with PTP1 (10uM) for 24h, **c.** after treating with PTP1 (100uM) for 24h, **d.** after treating with PTP3 (10uM) for 24h. and **e.** after treating with PTP3 (100uM) for 24h. Cells are stained with Annexin V and PI.*

PatuS cells were slight reduced after only 24 hours at a concentration of 10uM (PTP1 and PTP3).

Increasing the concentration of PTP1 to 100uM did not make much of a difference, while increasing the concentration of PTP3 to 100uM doubled the proportion of apoptotic cells, according to the FACS analysis.

4.4.5 PatuS treated with DMSO, 10uM PTP1, 100uM PTP1, 10uM PTP3 and 100uM PTP3 after **48 hours**

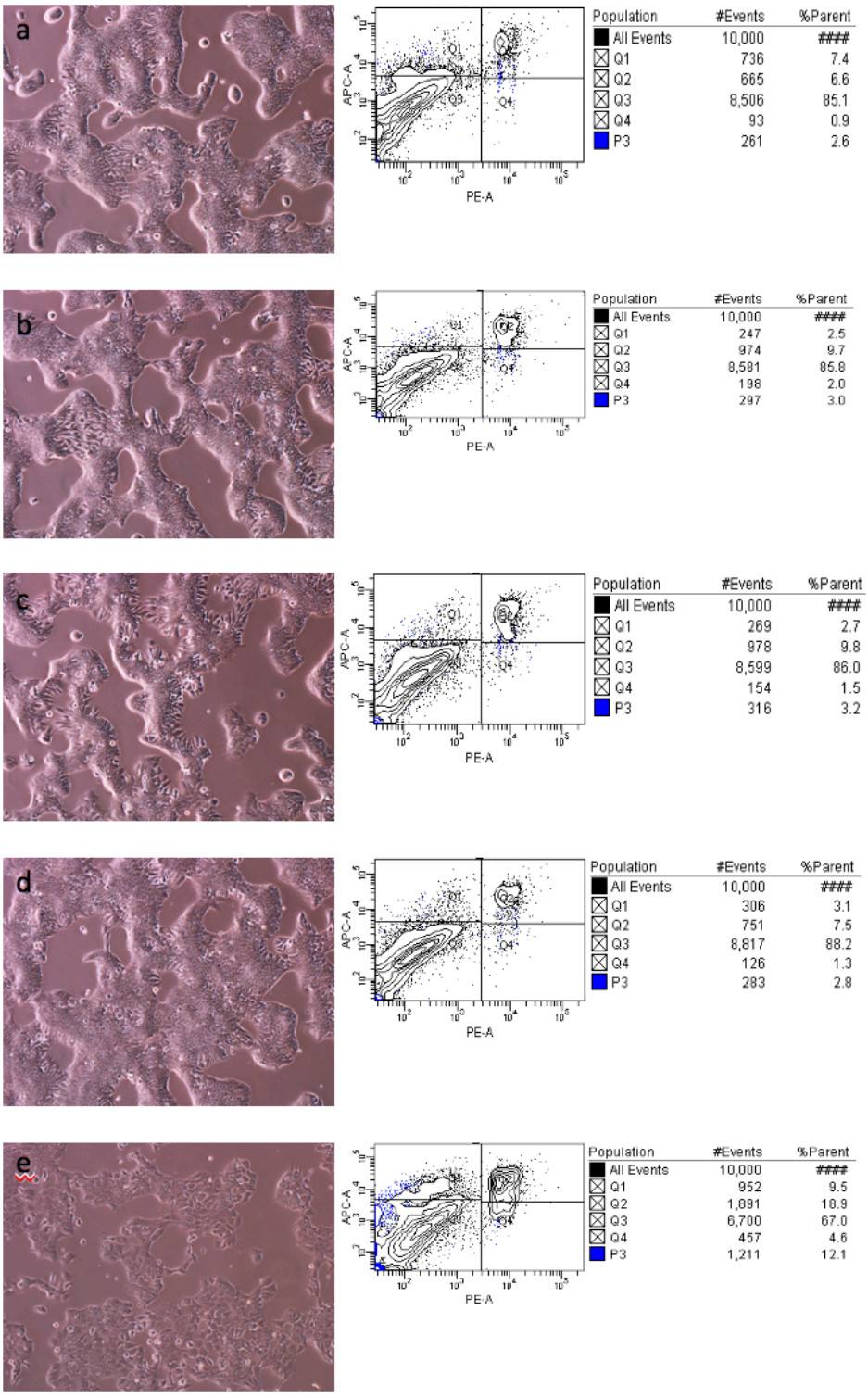

Figure 32a-e:
*LEFT: Microscopic picture of PatuS **a.** after treating with DMSO for 48h, **b.** after treating with PTP1 (10uM) for 48h, **c.** after treating with PTP1 (100uM) for 48h, **d.** after treating with PTP3 (10uM) for 48h and **e.** after treating with PTP3 (100uM) for 48h.*
*RIGHT: Flow cytometry of PatuS **a.** after treating with DMSO for 48h, **b.** after treating with PTP1 (10uM) for 48h, **c.** after treating with PTP1 (100uM) for 48h, **d.** after treating with PTP3 (10uM) for 48h. and **e.** after treating with PTP3 (100uM) for 48h. Cells are stained with Annexin V and PI.*

After 48 hours, even at a PTP concentration of 10uM, not only an increase in Q2 values but also changes in the appearance of the PatuS cells was observed.

This change in morphology was even stronger at higher concentration of PTPs. This effect was best to see after treating PatuS with PTP3 at a concentration of 100uM. The Q2 value was more than double compared to PTP3 at a concentration of 10uM and compared to DMSO-treated cells, and the cells released from their rather compact cell formation, making individual cells clearly visible.

4.4.6 PatuS treated with DMSO, 10uM PTP1, 100uM PTP1, 10uM PTP3 and 100uM PTP3 after **72 hours**

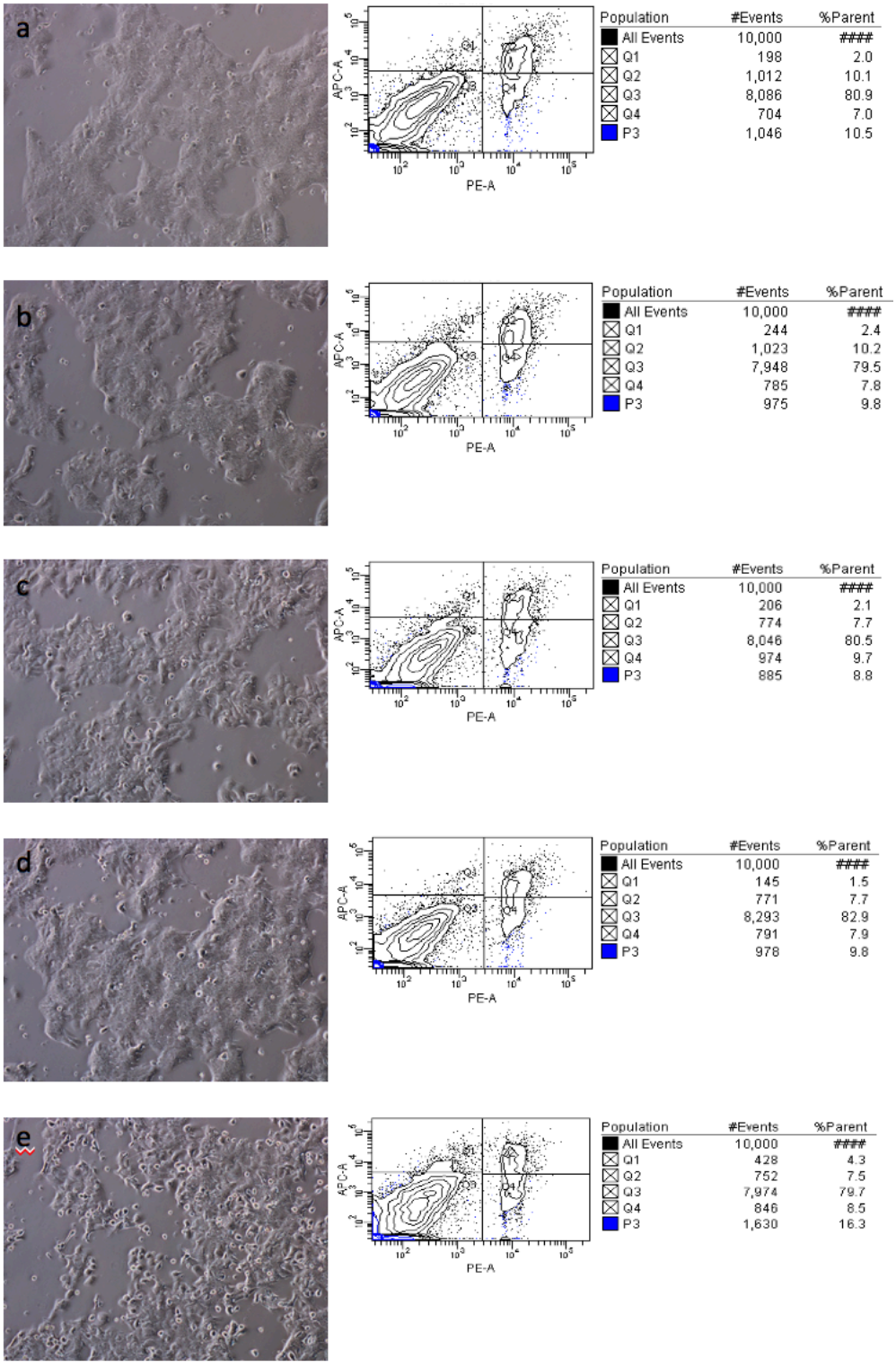

Figure 33a-e:
*LEFT: Microscopic picture of PatuS **a.** after treating with DMSO for 72h, **b.** after treating with PTP1 (10uM) for 72h, **c.** after treating with PTP1 (100uM) for 72h, **d.** after treating with PTP3 (10uM) for 72h and **e.** after treating with PTP3 (100uM) for 72h.*
*RIGHT: Flow cytometry of PatuS **a.** after treating with DMSO for 72h, **b.** after treating with PTP1 (10uM) for 72h, **c.** after treating with PTP1 (100uM) for 72h, **d.** after treating with PTP3 (10uM) for 72h. and **e.** after treating with PTP3 (100uM) for 72h. Cells are stained with Annexin V and PI*

The effect seen in the PatuS cells after 48 hours reverted after 72 hours. The treatments with PTP1 and PTP3 had the same or even less effect after 72 hours than the treatment with DMSO according to FACS.

4.4.7 Summary of FACS

In order to present the data of FACS in a clear manner, the data is displayed as a diagram (Figure 41-42).

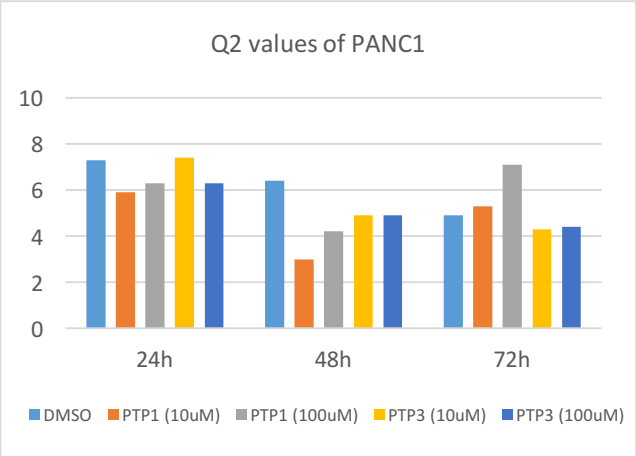

Figure 41: Q2 values of PANC1 after treating with DMSO, PTP1 (10uM, 100uM) and PTP3 (10uM, 100uM) to all time points.

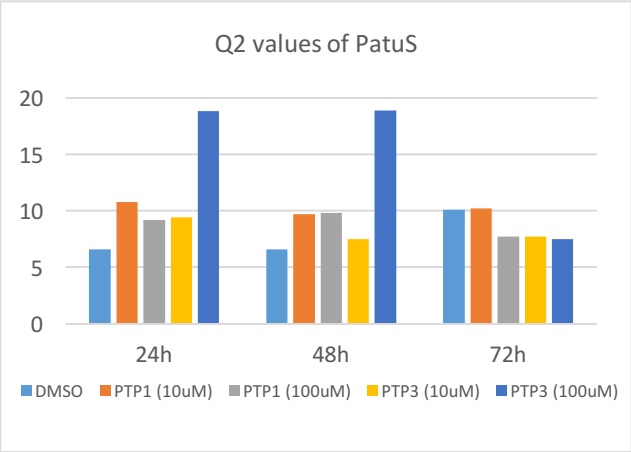

Figure 42: Q2 values of PatuS after treating with DMSO, PTP1 (10uM, 100uM) and PTP3 (10uM, 100uM) to all time points.

In the PANC1 cells, an increase in the concentrations of PTP1 and PTP3 lead to a small increase in apoptosis after 24 hours, 48 hours, and 72 hours. This suggests that the effect of PTPs in the PANC1 cells may be concentration-dependent.

In the PatuS cells, the Q2 value is highest after 24 hours and 48 hours at a concentration of 100µM PTP3. However, this effect was no longer visible after 72 hours, suggesting that the effect in the PatuS cells may be time-dependent.

4.5 Results of cell cycle analysis

To gain further insight into the mechanism of action of the bumetanide derivatives, cell cycle analysis was used to quantify the percentage of cells in each cell cycle phase. In this cell cycle analysis method, the fluorescent nucleic acid dye propidium iodide (PI) is used to determine the proportion of cells located in one of the three phases of the cell cycle.

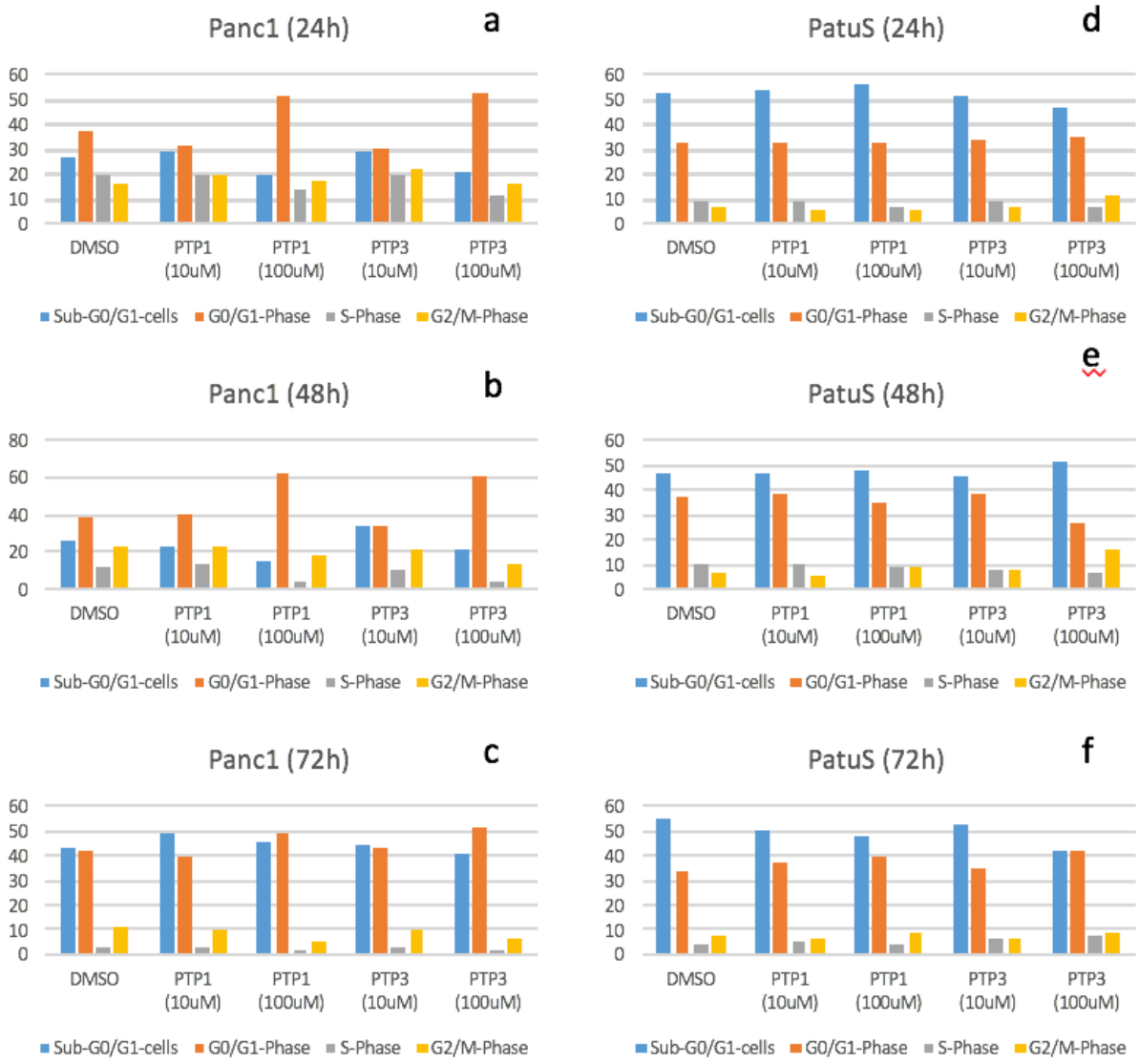

Figure 34: The amount of cells in %, which are in the individual phases of the cell cycle after treatment with DMSO, PTP1 (10uM, 100uM) and PTP3 (10uM, 100uM). The amount of PANC1 cells after 24 (**a**), 48 (**b**) and 72 hours (**c**). The amount of PatuS cells after 24 (**d**), 48 (**e**) and 72 hours (**f**). Cells in the sub-G0/G1-phase are considered apoptotic cells.

The PANC1 cells accumulated in the G1/G0 phase after treatment with 100uM PTP1 and PTP3 after 24 and 48 hours, however a concentration of 10uM of PTP1 or PTP3 had no effect on PANC1 cells. It looks like the PANC1 cells are arrested in G1/G0 after 48 hours. However, after 72 hours, it is visible that the amount of GO/G1 cells after treatment with PTP1 or PTP3 is the same as the amount of cells treated with DMSO, which proved that the cells were not blocked. Also the amount of dead cells increased significantly after 72 hours in all conditions, including DMSO-treated cells, suggesting that the cells were under some stress.

The PatuS cells were already rather stressed, as indicated by the high percentage of sub-G0 cells. When treated with 100uM PTP3 for 48 hours, however, they accumulated in the G2/M phase, which would induce a mitotic catastrophe, as cells are unable to complete mitosis. The amount of dead cells, however, was not markedly increased by extending treatment time, and the G2/M arrest was lost at the 72 hours time point.

5 DISCUSSION

PDAC is the fourth leading cause of cancer death in Japan, the US and Europe with a median survival rate of under 6 months and 5-year survival rate of 3 to 5%. This cancer's lethal nature stems from is rapidly dissemination to the lymphatic system and distant organs. Because of is aggressive biology it leads to a typical clinical presentation of incurable disease at the time of prognosis [3].
Current therapeutic strategies often have severe side effects due to insufficient selectivity, thereby worsening the patient's quality of life. Drug resistance is also an emerging issue. Furthermore, most treatments only prolong life for few months or even only weeks and do not provide a complete cure. As a result, new approaches in cancer therapy are eagerly needed.

In the context of this diploma thesis the question should be answered, if bumetanide derivatives have an effect on pancreatic ductal adenocarcinoma cells.

The results in general support the thesis that the derivatives have a mild cytostatic and cytotoxic effect on the cells used. So far, however, little is known about how the derivatives and to what extent contributes to the effect.

Among the derivatives used (PTP1, PTP2 and PTP3), PTP1 and PTPT3 showed a promising effect in both cell lines used (PANC1 and PatuS).

Therefore, among the tested derivatives, PTP1 and PTP3, in combination with a cytostatic drug, would be best for further study.

To see whether the derivatives have a synergistic effect in combination with well known chemotherapeutic agents (GEM, PTX and 5FU), a cytotoxicity assay was performed on the cell lines PANC1 and PatuS.

Especially the combination of PTP3 and GEM (10uM) seemed to show a small additive effect in PANC1 cells, which was confirmed by the t-test and analysis of variance.

Also recognizable due to the cytotoxicity assay is that the effects of PTP1 alone and PTP3 alone are approximately the same.

To confirm the results, and to understand the underlying mechanisms (i.e. whether PTPs are cytostatic or cytotoxic) the amount of apoptotic cells after treatment with PTP1 and PTP3 was determined by flow cytometry.

These studies showed that the PANC1 cells are clearly influenced only after a treatment time of 72 hours with both PTP1 and PTP3 at a concentration of 100uM.

For the PatuS cells, however, the treatment time of 72 hours seems to be too long and the cells might have adapted to the drug by that time. However, after 24 hours, but also after 48 hours, it was possible to observe an increase in apoptotic cells, especially after treatment with PTP3. Increasing the concentration from 10 to 100µM almost doubled the amount of apoptotic cells.

After cell cycle analysis, the PANC1 cells were found to accumulate in G0/G1 phase particularly upon treatment with 100uM PTP1 and PTP3 after 24 and 48 hours. After 72 hours hardly any cells can be detected in the S-phase.
In the PatuS cell line, on the other hand, a block in G2/M was observed after 48 hours treatment with 100uM PTP3, and some of the cells might fall into a state of mitotic catastrophe. In this experiment, however, a high proportion of cells were observed in the sub-G0 phase even in the control group, possibly indicating basal stress.

The apoptosis and cell cycle analyses were performed only once and should be repeated in the future, to confirm the results.

6 CONCLUSION AND FUTURE PROSPECTS

In summary, it has been shown that the bumetanide derivatives have a mild pro-apoptotic effect on the cell lines. However, whether this effect can be attributed to the NKCC1-cotransporters can not be said with 100% certainty but the experiments show a possible tendency in this direction. Irrespective of this, it might be worthwhile to further investigate the derivatives as a single active substance.
To what extent the PTPs induce cell death is still unclear.
Further experiments regarding the selectivity might give an indication of the exact mechanism of action. Likewise, the results obtained should be reproduced, since these are relatively uncharacterized substances.
In addition, a cross-inhibition of NKCC2 is to be investigated, since this represents an important transporter in the human body, which also effects other organs, like the heart and kidney.

The NKCC1-cotransporter appears to be a promising target in several studies. The transporter was also used in a study as a target for the possible inhibition of hepatocellular carcinoma [22].
But also for neurological and psychiatric diseases, the NKCC1-cotransporter might be interesting [23].
The PTPs can also be tested on other cancer cells for these aspects.

7 ABSTRACT

PTP1, PTP2 and PTP3 are derivatives of bumetanide, a loop diuretic commonly used in heart failure. They are predicted to inhibit the NKCC-cotransporter, as does bumetanide. In particular, the NKCC1 isoform has become increasingly important in cancer research in recent years. As the current therapies for cancer are experiencing severe side effects and drug-resistance is on the rise, the synthesis of new drugs is eagerly needed.

This thesis aims to verify the assumption that the bumetanide derivatives have a cytotoxic or cytostatic effect on pancreatic ductal adenocarcinoma (PDAC) cell lines (PANC1 and PatuS), due to inhibition of NKCC1-transporters.

Therefore, the PTPs were tested on PANC1 and PatuS cell lines alone as well as in combination with gemcitabine, paclitaxel and 5-fluorouracil, which are well-known drugs used in cancer therapy of PDAC. After 72 hours of treatment, cell death was induced by PTP1 and PTP3 in some conditions. Further investigations in combination with GEM, PTX and 5-FU were performed, whereby the combination of PTP3 and GEM indicates a possible additive effect.

Annexin V and PI staining were performed in order to investigate the specific effect of PTPs. In PANC1 cells there was an increase in apoptotic cells after 72 hours of treatment with PTP1 and PTP3. In PatuS cells however, 72 hours of treatment result in a lower apoptotic rate than after 24 or 48 hours of treatment.

After staining the DNA with PI to detect the amount of cells in each cell cycle phase, it was seen that PANC1 cells are already arrested after 48 hours of treatment with PTP1 and PTP3 in the cell cycle. In PatuS cells, some of the cells might undergo mitotic catastrophe.

Further studies are necessary to evaluate the potential of PTPs as anticancer drugs.

PTP1, PTP2 und PTP3 sind Derivate von Bumetanid, einem bei Herzinsuffizienz häufig verwendeten Schleifendiuretikum. Es wird angenommen, dass diese Derivate, ebenso wie Bumetanid, den NKCC-Transporter hemmen. Insbesondere die NKCC1-Isoform hat in der Krebsforschung in den letzten Jahren an Bedeutung gewonnen. Da die derzeitigen Krebstherapien schwerwiegende Nebenwirkungen haben und die Arzneimittelresistenz zunimmt, ist die Synthese neuer Arzneimittel dringend erforderlich.

Die vorliegende Arbeit soll die Annahme bestätigen, dass die Bumetanid-Derivate aufgrund der Hemmung von NKCC1-Transportern eine zytotoxische oder zytostatische Wirkung auf Adenokarzinom (PDAC) -Zelllinien des Pankreasgangsystems (PANC1 und PatuS) haben.
Daher wurden die PTPs auf PANC1- und PatuS-Zelllinien allein, sowie in Kombination mit Gemcitabin, Paclitaxel und 5-Fluorouracil getestet, die als Arzneimittel zur Krebstherapie von PDAC von Bedeutung sind. Nach 72-stündiger Behandlung wurde der Zelltod unter bestimmten Bedingungen durch PTP1 und PTP3 induziert. Weitere Untersuchungen in Kombination mit GEM, PTX und 5-FU wurden durchgeführt, wobei die Kombination von PTP3 und GEM einen möglichen additiven Effekt anzeigt.
Annexin V- und PI-Färbung wurden durchgeführt, um die spezifische Wirkung von PTPs zu untersuchen. In PANC1-Zellen war nach 72-stündiger Behandlung mit PTP1 und PTP3 ein Anstieg anapoptotischen Zellen zu verzeichnen. In PatuS-Zellen führen 72 Stunden Behandlung jedoch zu einer niedrigeren Apoptoserate als nach 24 oder 48 Stunden Behandlung.
Nach dem Färben der DNA mit PI zum Nachweis der Zellmenge in jeder Zellzyklusphase wurde festgestellt, dass PANC1-Zellen bereits nach 48-stündiger Behandlung mit PTP1 und PTP3 im Zellzyklus angehalten wurden. In PatuS-Zellen erleiden einige der Zellen eine mitotische Katastrophe.
In Zukunft sind weitere Studien erforderlich, um das Potenzial von PTPs als Krebsmedikamente zu bewerten.

8 REFERENCES

1. American Cancer Society. What Is Pancreatic Cancer? 2016-05-31. doi:10.1016/j.geomphys.2011.12.017
2. staff B co., Staff B co. Medical gallery of Blausen Medical 2014. *WikiJournal Med*. 2014;1(2):10. doi:10.15347/wjm/2014.010
3. Hezel AF, Kimmelman AC, Taguchi R, Stanger BZ, Bardeesy N, Depinho R a. Genetics and biology of pancreatic ductal adenocarcinoma. *Genes Dev*. 2006;20(10):1218-1249. doi:10.1101/gad.1415606
4. Siegel RL, Miller KD, Jemal A. Cancer statistics, 2018. *CA Cancer J Clin*. 2018;68(1):7-30. doi:10.3322/caac.21442
5. Heinmöller E, Gaumann A, Ott C, Klebl F, Schölmerich J. Intraepitheliale Neoplasien (PanIN) und intraduktale papillär-muzinöse Neoplasien (IPMN) des Pankreas als Vorläufer des PankreaskarzinomsIntraepithelial Neoplasms (PanIN) and Intraductal Papillary-Mucinous Neoplasms (IPMN) of the Pancreas as Precursor Les. *Med Klin*. 2007;102(2):127-135. doi:10.1007/s00063-007-1013-8
6. Lal G, Liu L, Hogg D, Lassam NJ, Redston MS, Gallinger S. Patients with both pancreatic adenocarcinoma and melanoma may harbor germlineCDKN2A mutations. *Genes, Chromosom Cancer*. 2000;27(4):358-361. doi:10.1002/(SICI)1098-2264(200004)27:4<358::AID-GCC4>3.0.CO;2-O
7. Bumetanide | C17H20N2O5S - PubChem. https://pubchem.ncbi.nlm.nih.gov/compound/bumetanide#section=Top. Accessed February 20, 2019.
8. Russell JM. Sodium-Potassium-Chloride Cotransport. *Physiol Rev*. 2017;80(1):211-276. doi:10.1152/physrev.2000.80.1.211
9. GTEx Project. GTEx portal. GTEx Analysis Release V6p (dbGaP Accession phs000424.v6.p1). doi:10.1038/86850
10. WANG X, KUAI Q, REN S, et al. Synergistic antitumor activity of gemcitabine combined with triptolide in pancreatic cancer cells. *Oncol Lett*. 2016;11(5):3527-3533. doi:10.3892/ol.2016.4379
11. Mini E, Nobili S, Caciagli B, Landini I, Mazzei T. Cellular pharmacology of gemcitabine. *Ann Oncol*. 2006;17(SUPPL. 5):v7-v12. doi:10.1093/annonc/mdj941
12. Minoguchi M, Tanno S, Okumura T, et al. Gemcitabine chemoresistance and molecular markers associated with gemcitabine transport and metabolism in human pancreatic cancer cells. *Br J Cancer*. 2007;96(3):457-463. doi:10.1038/sj.bjc.6603559
13. Horwitz SB. Taxol (paclitaxel): mechanisms of action. *Ann Oncol Off J Eur Soc Med Oncol*. 1994;5 Suppl 6:S3-6. http://www.ncbi.nlm.nih.gov/pubmed/7865431. Accessed February 20, 2019.
14. Abcam. Counting cells using a hemocytometer. *Protocols*. 2015;000:4-5. doi:10.1038/sj.ejhg.5200954
15. Abcam. Flow cytometry introduction | Abcam. Abcam. https://www.abcam.com/protocols/introduction-to-flow-cytometry. Published 2018. Accessed February 22, 2019.
16. Biosciences BD, Hingorani R, Deng J, Elia J, Mcintyre C, Mittar D. *Application Note Detection of Apoptosis Using the BD Annexin V FITC Assay on the BD FACSVerse™ System*.; 2011.

https://www.bdbiosciences.com/documents/BD_FACSVerse_Apoptosis_Detection_AppNote.pdf. Accessed February 22, 2019.
17. Abcam. Propidium Iodide Flow Cytometry Kit for Cell Cycle Analysis. Abcam. https://www.abcam.com/protocols/flow-cytometric-analysis-of-cell-cycle-with-propidium-iodide-dna-staining. Published 2012. Accessed February 22, 2019.
18. Broad Institute Cancer Cell Line Encyclopedia (CCLE). portals.broadinstitute.org. https://portals.broadinstitute.org/ccle. Accessed February 11, 2019.
19. DNEbM. Glossar zur Evidenzbasierten Medizin. *Dtsch Netzw Evidenzbasierte Medizin eV*. 2011:61. http://www.ebm-netzwerk.de/grundlagen/images/dnebm-glossar-2011.pdf [Online. Letzter Zugriff:29/12/2011].
20. Kim TK. KOREAN J ANESTHESIOL. *Korean J Anesth*. 2017;70(1):22-26. doi:https://doi.org/10.4097/kjae.2017.70.1.22
21. Distelhorst CW. Apoptosis. *Calcium Signaling, Second Ed*. 2005;44(0):433-454. doi:10.1201/9781420038231
22. Hao N, Xu C, Chen N, et al. Discovery of NKCC1 as a potential therapeutic target to inhibit hepatocellular carcinoma cell growth and metastasis. *Oncotarget*. 2017;8(39):66328-66342. doi:10.18632/oncotarget.20240
23. Ben-Ari Y. NKCC1 Chloride Importer Antagonists Attenuate Many Neurological and Psychiatric Disorders. *Trends Neurosci*. 2017;40(9):536-554. doi:10.1016/j.tins.2017.07.001
24. Gstraunthaler G, Lindl T. *Zell- Und Gewebekultur: Allgemeine Grundlagen Und Spezielle Anwendungen*. 7. Auflage. Medizinische Universität Innsbruck, Innsbruck, Germany: Springer Spektrum; 2013. doi:10.1007/978-3-642-35997-2

I. List of figures

II. List of schemes

III. List of tables